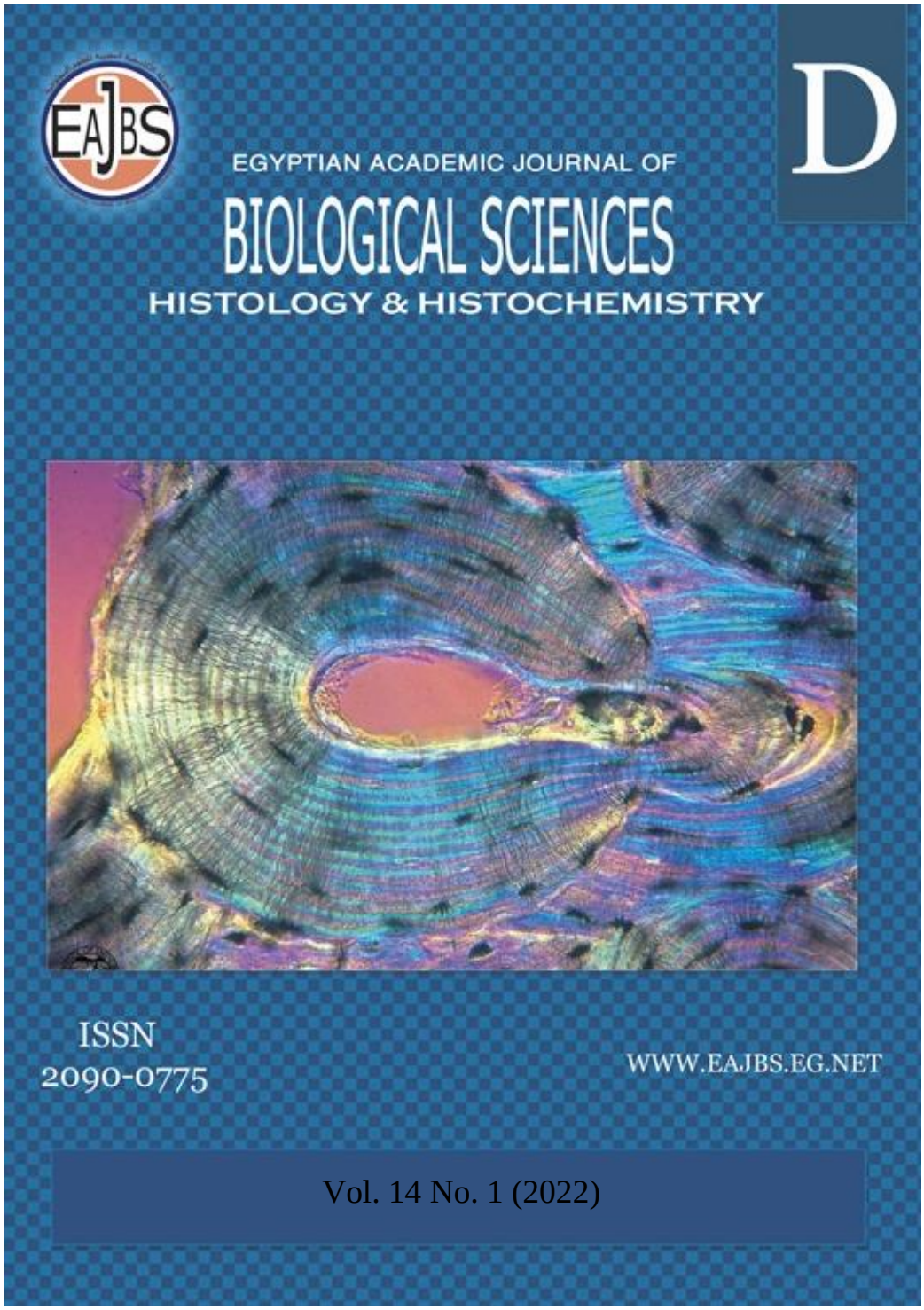

Citation: Egypt. *Acad. J. Biolog. Sci. (D-Histology and histochemistry) Vol.14(1) pp1-25(2021)*
DOI: 10.21608/EAJBSD.2022.214866

Egypt. Acad. J. Biolog. Sci., 14(1): 1-25 (2022)

Egyptian Academic Journal of Biological Sciences
D. Histology & Histochemistry
ISSN 2090 – 0775
http://eajbsd.journals.ekb.eg

Effect of Exenatide on Apoptosis, Autophagy, and Necroptosis in the Hippocampus of STZ-Induced Diabetic Female Rats: An Immunohistochemical Study

Eman M. Elsaeed[1], Ahmed G. A. Hamad[2], Omnia S. Erfan[2], Mona A. El-Shahat[2] and Fathy A. Ebrahim[2]

1-Human Anatomy and Embryology, Faculty of Medicine, Port Said University, Egypt.

2-Human Anatomy and Embryology, Faculty of Medicine, Mansoura University, Egypt.

E.Mail: Eman.Mohamed@med.psu.edu.eg - a.gamal491@gmail.com - Ominasameer@mans.edu.eg - shahat111@mans.edu.eg - dr_fathy@mans.edu.eg

ARTICLE INFO

Article History
Received:23/12/2021
Accepted:17/1/2022
Available:19/1/2022

***Keywords*:**
Diabetes, exenatide, apoptosis, autophagy, necroptosis.

ABSTRACT

Introduction: Diabetes mellitus has serious consequences on all body systems, and the hippocampus is a vulnerable site for this affection. The study aims to examine the effect of exenatide treatment on the diabetic rats` hippocampal oxidative stress, apoptosis, autophagy, and necroptosis. ***Materials and methods*:** Twenty-four adult female albino rats were divided into four groups: control, diabetic (received a single intraperitoneal injection of streptozotocin (STZ) at a dose of 45 mg/kg), treated (received a single intraperitoneal injection of STZ and daily intraperitoneal injection of exenatide at a dose of 1 µg/kg for 10 weeks), and exenatide (received daily intraperitoneal injection of exenatide for 10 weeks). After 10 weeks, blood samples were collected for measuring blood glucose levels, and hippocampi were dissected out. Tissue homogenates of the hippocampus from one hemisphere were used for oxidative stress markers. The other hemisphere was processed for histopathological and immunohistochemical stain using caspase 3, microtubule-associated protein light chain 3 (LC3b), p62, and receptor-interacting kinase (RIP3) antibodies. ***Results*:** Oxidative stress was evident in the diabetic hippocampus, with insignificant improvement with exenatide treatment. Apoptosis was detected in CA1, CA3, and dentate gyrus (DG), and significant improvement was noticed with exenatide treatment mainly in DG. Autophagy was impaired in all hippocampal regions, and exenatide significantly improved its activity. Necroptosis was detected mainly in diabetic CA1, although not significant when compared with other groups. ***Conclusion*:** Histopathological improvement resulting from exenatide treatment is mainly due to reducing hippocampal neuronal apoptosis and restoring autophagy, while the effect on necroptosis was non-significant.

INTRODUCTION

Diabetes mellitus (DM) signifies a major public health burden, as it is predicted to increase in prevalence from 463 million in 2019 to 700 million in 2045 according to the International Diabetes Federation (IDF) (Saeedi *et al.,* 2019)**.**

Chronic hyperglycemia represents the main injurious mechanism in all types of diabetes (Forbes and Cooper, 2013). Hyperglycemia is reported to increase oxidative stress, neuroinflammation, and mitochondrial dysfunction, and impair neuronal integrity leading to neurodegeneration (González-Reyes *et al.,* 2016 & Lee *et al.,* 2018). Furthermore, patients of all ages with uncontrolled diabetes are at high risk to develop cognitive impairment and considerable hippocampal atrophy (Fotuhi *et al.,* 2012).

Hippocampus has a role in memory, spatial navigation, emotional behavior, and regulation of hypothalamic functions (Anand and Dhikav, 2012). Cognitive decline is regarded as one of the most common diabetic brain complications. Multiple meta-analyses reported that diabetes is associated with lower cognitive performance in children with type 1 DM, and increased risk for dementia, which are considered some phenotypes of "geriatric syndromes" in older patients (Gaudieri *et al.,* 2008 & Lu *et al.,* 2009). Crosstalk between DM and Alzheimer's disease (AD) has been proved, and the term "type 3 diabetes" has emerged defining insulin resistance-induced AD (Maher and Schubert, 2009 & Baglietto-Vargas *et al.,* 2016). Further research has found epidemiological associations and common pathophysiological mechanisms between the two diseases (Li *et al.,* 2015).

Autophagy, necroptosis, and apoptosis are kinds of cellular death with different functions. Apoptosis is an active, tightly regulated, metabolic, and genetically encoded form of cell death (Elmore, 2007). It is reported to be upregulated in neurodegenerative diseases (Singh et al., 2019). Over-stimulation of autophagy can convert it to a pro-death rather than a pro-survival mechanism causing the cells to progress to autophagic cell death (Yang *et al.,* 2017). Necroptosis is a programmed method of inflammatory cell death, whereas apoptosis is a programmed method of non-inflammatory cell death (Zhang *et al.,* 2018). Both apoptosis and necroptosis play significant roles in the progression of diabetic complications, as they may culminate in tissue injuries in the kidneys, retina, heart, and nervous system (Volpe *et al.,* 2018). RIPK1, which is an initiating factor for necroptosis activation, has been implicated in neurodegeneration based on studies in human postmortem tissue (Yuan *et al.,* 2019a). Activated RIP1 recruits RIP3, which is phosphorylated and ubiquitinated. Although RIP1 and RIP3 are important for induction of necroptosis, overexpression of RIP3 alone can induce necroptosis by a mechanism independent of its kinase activity (Chen *et al.,* 2019).

Exenatide is a member of a class of anti-diabetic drugs that act as glucagon-like peptide-1 (GLP1) agonists (Davidson *et al.,* 2005). GLP1 modulates insulin release by enhancing glucose-dependent insulin secretion. Although GLP1 receptors are principally located in pancreatic islets, they are largely expressed throughout the body including the hippocampus (Gumuslu *et al.,* 2018). Remarkably, exenatide has been reported to induce neuronal progenitor cell proliferation and increase neurogenesis in mouse brains (Hamilton *et al.,* 2011). Moreover, in animal studies, the drug has been shown to enhance synaptic plasticity and cognitive performance (McClean *et al.,* 2010). For these reasons, exenatide has been proposed as a therapeutic agent in neurological conditions like Parkinson's disease

(PD) and Alzheimer's disease (AD) (McGhee *et al.*, 2016).

Up to our knowledge, there are no studies on the role of exenatide on diabetic brain necroptosis. This study was conducted to detect the effect of exenatide on diabetic rats` hippocampal oxidative stress, apoptosis, autophagy, and necroptosis and its ability to alleviate the diabetic medicated pathology.

MATERIALS AND METHODS

Experimental Animals:

Animals were housed in agreement with the regulations approved by the committee of animals' experimentation of Mansoura University, and the study was approved by the Institutional Review Board of Mansoura University, faculty of medicine. Twenty-four adult female albino rats (150-200 grams, aged around 2 months) were housed in an experimental research center, acclimatized for two weeks, and fed on a commercial basal *ad libitum* diet and tap water.

Drugs and Chemicals:

Streptozotocin was purchased from Sigma Aldrich, Germany, No. S0130. Exenatide (prefilled pen, 10 mcg solution) was purchased from Eli Lilly Company, Egypt. Kits for reduced glutathione (GSH), superoxide dismutase (SOD), and malondialdehyde (MDA) oxidative stress markers were purchased from Biodiagnostic Company, Elomraniya, Egypt. The rabbit polyclonal anti-caspase-3 antibody was purchased from Servicebio, China, GB11532. The rabbit polyclonal anti-LC3b antibody was purchased from Abcam, UK, No. ab48394. The rabbit polyclonal anti-p62 antibody was purchased from Sigma Aldrich, Germany, No. SAB5700845. The rabbit polyclonal anti-RIP3 antibody was purchased from Sigma Aldrich, Germany, No. PRS2283. The biotin-labelled secondary antibody rabbit anti-rat IgG was purchased from Boster Biological Technology, USA, No. BA1005.

Experimental Design:

Rats were randomly assigned to 4 groups each with 6 rats. Group 1 (control) received a single intraperitoneal injection of 1 mL saline. Group 2 (diabetic) received a single intraperitoneal injection of STZ (freshly dissolved in citrate buffer 0.5 M, pH 4.5) at a dose of 45 mg/kg (Mostafavinia et al., 2016), and was confirmed 5 days later when blood glucose level was ≥ 200 mg/dl (Qinna and Badwan, 2015). Group 3 (treated) received a single intraperitoneal injection of STZ at a dose of 45 mg/kg, and after diabetes was confirmed, exenatide was administered daily by intraperitoneal injection at a dose of 1 µg/kg for 10 weeks (Lotfy et al., 2014). Group 4 (exenatide) received exenatide at a dose of 1 µg/kg for 10 weeks.

Samples Collection:

1. Blood Samples:

After 5 days of STZ administration, animals were anaesthetized by diethyl ether, and blood samples were collected via tail vein puncture for measuring blood glucose levels. After 5 weeks of diabetes confirmation, blood samples were collected for following up. At the end of the experiment after 10 weeks of diabetes confirmation, animals were anaesthetized by diethyl ether, and blood samples were collected via intracardiac catheter for measuring blood glucose levels.

2. Brain Tissue Collection:

After obtaining blood samples, animals were decapitated and brains were dissected out and washed. The brain was bisected in the midline and the hippocampus of the right hemisphere was dissected out for performing tissue homogenates for measuring oxidative stress markers. The other hemisphere was processed for histopathological and immunohistochemical studies.

Biochemical Studies:

1. Blood Glucose Level:

Blood glucose level was measured by the glucose oxidase

method (Buzanovskii, 2015). It was measured after 5 days to confirm DM, then it was measured after 5 weeks and at the end of the experiment (10 weeks).

2. Oxidative Stress Markers:

Preparation of hippocampal homogenate was done in receptor isolation buffer using a Teflon pestle tissue grinder. It was centrifuged at 12,000×g for 20 min at 2°C, and the supernatant was recuperated, kept on ice, and filtered on a 0.2 µm membrane filter. Then, it was diluted, mixed with E2-A-FITC reagent, and incubated at room temperature for 30–60 min. The mixture was centrifuged at 10,000×g at 4°C for 15–30 min. The bound reagent was retained on the membrane filter, whereas the free reagent passed through it. A microplate reader at 485 nm excitation and 512 nm emission was used for measuring the fluorescence associated with the membrane or in the eluate. For measuring on the membrane, the material was recuperated by 100 µL of PBS and resuspended by repeated pipetting or purged with 20 % DMSO in water. For measuring in the eluate, the inverse relationship of fluorescein was a measure of reagent binding to cytosolic proteins (Gagne, 2014). After hippocampal homogenate was prepared, activities of MDA, SOD, and GSH oxidative stress markers were examined using the corresponding kit according to the manufacturer's instructions.

Histopathological Studies:

Tissues were fixed in 10% phosphate-buffered formalin to be processed by histopathological techniques. They were dehydrated using ascending graded concentrations of alcohol, cleared in xylene, and embedded in soft then hard paraffin wax. Using a rotatory microtome, coronal sections were cut in the dorsal hippocampus at a thickness of 5-6µm and mounted on slides for staining. They were stained by Nissl stain (toluidine blue stain) as previously described (Culling, 2013).

Immunohistochemical Studies:

The prepared paraffin sections were deparaffinized using xylene, rehydrated, and 0.03 % hydrogen peroxide was added to block endogenous peroxidase activity. Sections were boiled in 0.01 M citrate buffer (pH 6) to unmask the antigenic site and incubated in PBS to avoid nonspecific binding. The diluted primary antibodies for caspase-3 (1:500), LC3b (1:400), p62 (1:200), and RIP3 (1:200) were added and incubated overnight at 4 ◦C. After incubation and washing in PBS, the second biotin-labeled anti-rabbit IgG was added. Sections were incubated with DAB for 5 minutes. Finally, slides were washed in PBS and counterstained with hematoxylin (Ramos-Vara, 2005).

Image Analysis:

Four distributed sections were taken from each animal in each group for performing image analysis. Slides were photographed using an Olympus® microscope with a ½ X photo adaptor attached to a digital camera and connected to a PC. For each slide, images were taken from the CA1 region, CA3 region, and upper limb of the DG region (figure 2A) using a 40× objective (area: 0.07 mm^2). Images were analyzed using the public domain of ImageJ, a Java-based image processing computer program, with a built-in routine for stain quantification measuring area fraction, and for counting cells. For measuring area fraction in immune-stained sections, hematoxylin and DAB (for locating the antigen of interest) were digitally separated using the color deconvolution method. Using threshold adjustment, areas of intense brownish coloration were selected in the DAB image and measured as area fractions. For counting toluidine blue-stained cells, neurons of CA1, CA3, and DG that show vesicular nuclei were counted. Glial cells and cells showing nuclear fragmentation or pyknosis were excluded.

Statistical Analysis:

Data were collected and analyzed using the computer program SPSS version 20. They were calculated in the form of mean and standard deviation (SD). One-way ANOVA test was used for detecting if there were significant differences between groups, and the post-hoc Tukey's test was used for comparing values between every two independent groups. *P*-value ≤ 0.05 was considered statistically significant.

RESULTS

Blood Glucose Levels:

After 5 days of STZ injection, rats in diabetic and treated groups were proved to be diabetics with no statistically significant difference (p=0.522). Throughout the experiment and at its end, there was a statistically significant difference between the control group and these two groups. In addition, the treated group showed a statistically significant decrease in blood glucose level when compared with the diabetic group after 5 weeks (p=0.025) and after 10 weeks(p=0.004) (Fig. 1).

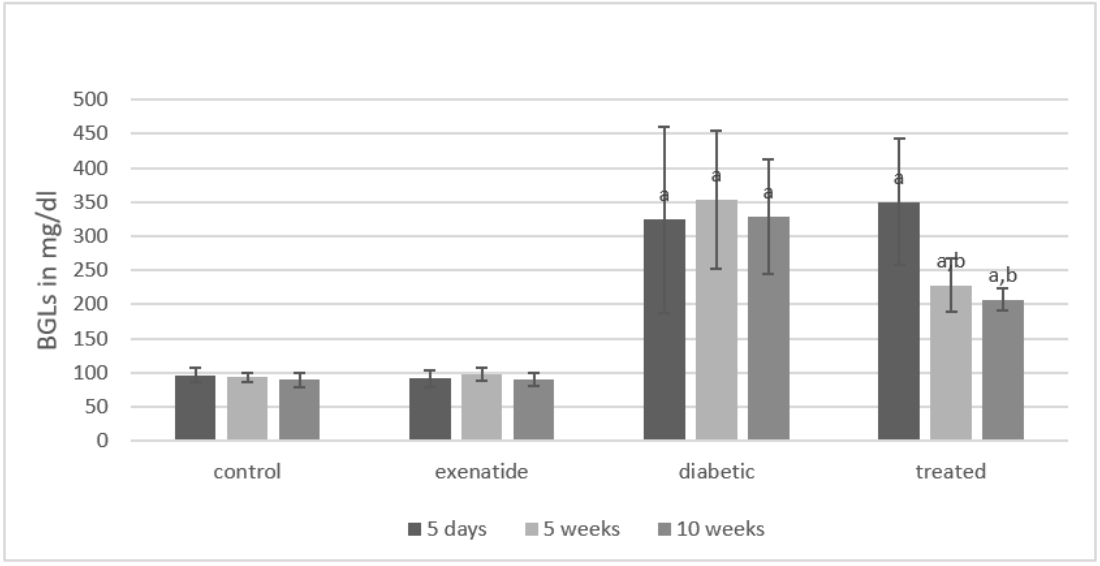

Fig. 1. Mean ±SD values of blood glucose levels after 5 days of STZ administration, 5 weeks and 10 weeks of diabetes confirmation. [a] Significantly different from the control group. [b] Significantly different from the diabetic group.

Oxidative Stress Markers:

There were statistically significant differences between control and diabetic groups in oxidative stress markers (MDA, SOD, and GSH) (p=0.004). In comparing control and treated groups, there was a statistically significant difference in SOD activity (p=0.025), and other oxidative stress markers (p=0.004). However, oxidative stress markers in the treated group were not statistically different from the diabetic group (**Table 1**).

Table 1. Values of mean and standard deviation for oxidative stress markers in tissue homogenate of the hippocampus of the different groups.

Group	SOD u/gm mean±SD	GSH mmol/g mean±SD	MDA mmol/g mean±SD
Control	81.72±1.55	15.04±5.66	1.54±0.42
Diabetic	92.24[a]±7.14	6.44[a]±1.2	2.87[a]±0.43
Treated	87.76[a]±8.26	6.48[a]±1.36	2.68[a]±0.38
Exenatide	80.69±1.71	14.82±7.2	1.37±0.36

[a] Significantly different from the control group.

Toluidine Blue-Stained Sections:

The control and the exenatide groups showed normal architecture of the hippocampus consisting of CA1 and CA2 related to the lateral ventricle, and the dentate gyrus surrounded CA3 and CA4 (Fig. 2B). The pyramidal neurons of CA1 (Figs. 3A, 3D), CA3 (Figs. 4A, 4D), and granular cell of DG (Figs. 5A, 5D) showed normal vesicular nuclei and compact arrangement.

The diabetic group showed few darkly-stained shrunken cells in the small pyramidal cell layer of CA1 (Fig. 3B) and the large pyramidal cell layer of CA3 (Fig. 4B). On the other hand, many darkly-stained shrunken cells were observed in the granular layer of DG (Fig. 5B). As compared to the control group, a statistically significant decrease in cell count existed in CA1, CA3, and DG regions (P<0.0005) (Fig. 6).

The treated group showed few darkly-stained neurons in CA1 (Fig. 3C) and DG (5C). As compared to the control group, a statistically significant decrease in cell count was detected in CA1, CA3, and DG (P<0.0005). However, a statistically significant increase in cell count existed in CA1, and DG (P<0.0005) as compared to the diabetic group (Fig. 6).

Caspase 3 Stained Sections:

The active cleaved anti-caspase 3 antibodies showed weak immune-reactivity in hippocampal neuronal processes of the control and exenatide groups in CA1 (Figs. 7A, 7D), CA3 (Figs. 8A, 8D), and DG (Figs. 9A, 9D). The diabetic group showed more intense immune-reactivity of neuronal processes (figure 8B, 9B). The area fraction of intense immune stain increased significantly in CA3 and DG (P<0.0005), as compared to the control group (Fig. 10). The treated group showed less intense immune-reactivity as compared to the diabetic group mainly in DG (Fig. 9C) that was revealed in a statistically significant decrease in measured area fraction (P<0.0005). The DG in the treated group was comparable to the control group as non-significant differences existed in area fraction (P=0.192) (**Fig. 10**).

LC3b and p62 Stained Sections:

Both control and exenatide groups showed weak immune-expression of LC3b and p62 in the cytoplasm of pyramidal neurons in CA1and CA3 and granular neurons in DG. The diabetic group showed more intense immune-reaction of LC3b in CA1 (fig. 11B), CA3 (Fig. 12B), and DG (Fig. 13B) as compared to the control group; with a statistically significant increase in area fractions of CA1, CA3, and DG (P<0.0005) (Fig. 14). Also, the diabetic group exhibited associated increased immune-reaction of p62 in CA1(Fig. 15B), CA3 (Fig. 16B), and DG (Fig. 17B).

The treated group showed less intense immune-reaction of LC3b in CA1 (Fig. 11C), CA3 (Fig. 12C), and DG (figure 13C) as compared to the diabetic group; with a statistically significant decrease in area fractions for CA1, CA3, and DG (Fig. 14). For p62, the treated group showed a statistically significant decrease in area fractions of CA1 (Fig. 15C) (P=0.049), CA3 (figure 16C), and DG (figure 17C) (P<0.0005) when compared to the diabetic group (Fig. 18).

RIP3 Stained Sections:

The control and the exenatide groups revealed weak immune-expression of RIP3 in the cytoplasm of neurons and neuronal processes in CA1 (Fig. 19A) then DG (Fig. 21A), and least detected in CA3 (Fig. 20A). The diabetic group showed increased immune-reaction mostly in CA1 (Fig. 19B) and DG (Fig. 21B), with no statistically significant differences (P>0.05) from the control group. The treated group as well showed a positive immune reaction in CA1 (fig. 19C), but not statistically significant from the control or diabetic groups (Fig. 22).

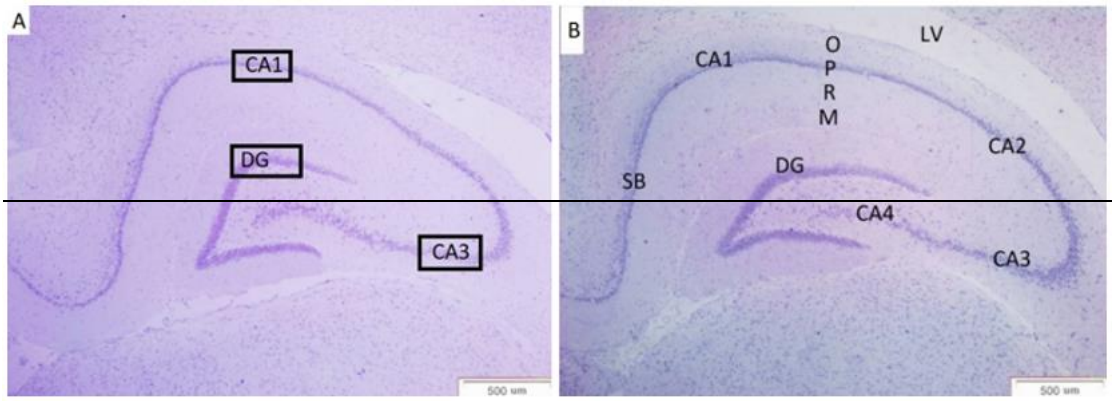

Fig. 2. Toluidine blue-stained coronal sections from rat hippocampus of the control group. (A) hippocampal level in cut sections & areas used for higher magnification and quantification. (B) CA1 and CA2 are related to the lateral ventricle (LV), the dentate gyrus (DG) surrounding CA3 and CA4. Layers of the hippocampus proper include the molecular layer (M), striatum radiatum (R), pyramidal layer (P), and striatum oriens (O)& (SB) subiculum. X40 magnification.

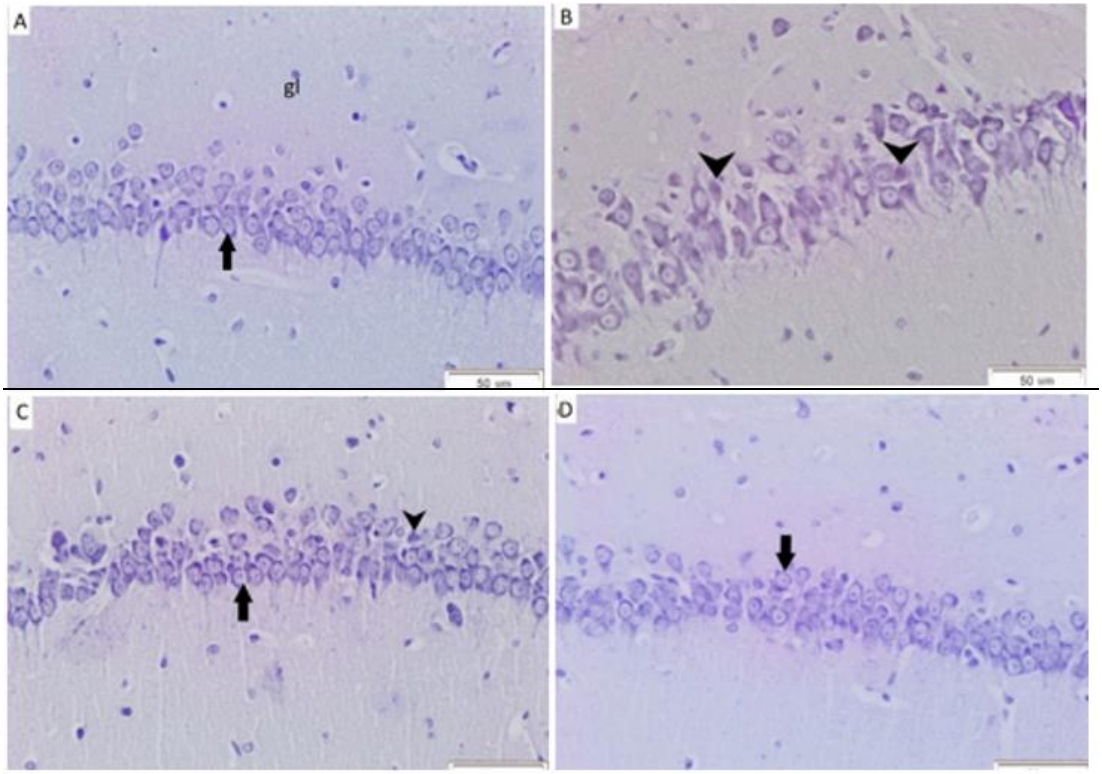

Fig. 3. Toluidine blue-stained coronal sections show small pyramidal cells of CA1 in (A) control, (B) diabetic, (C) treated &(D) exenatide groups respectively (arrows). Arrowheads point to darkly-stained shrunken neurons. (gl) glial cells. X400 magnification.

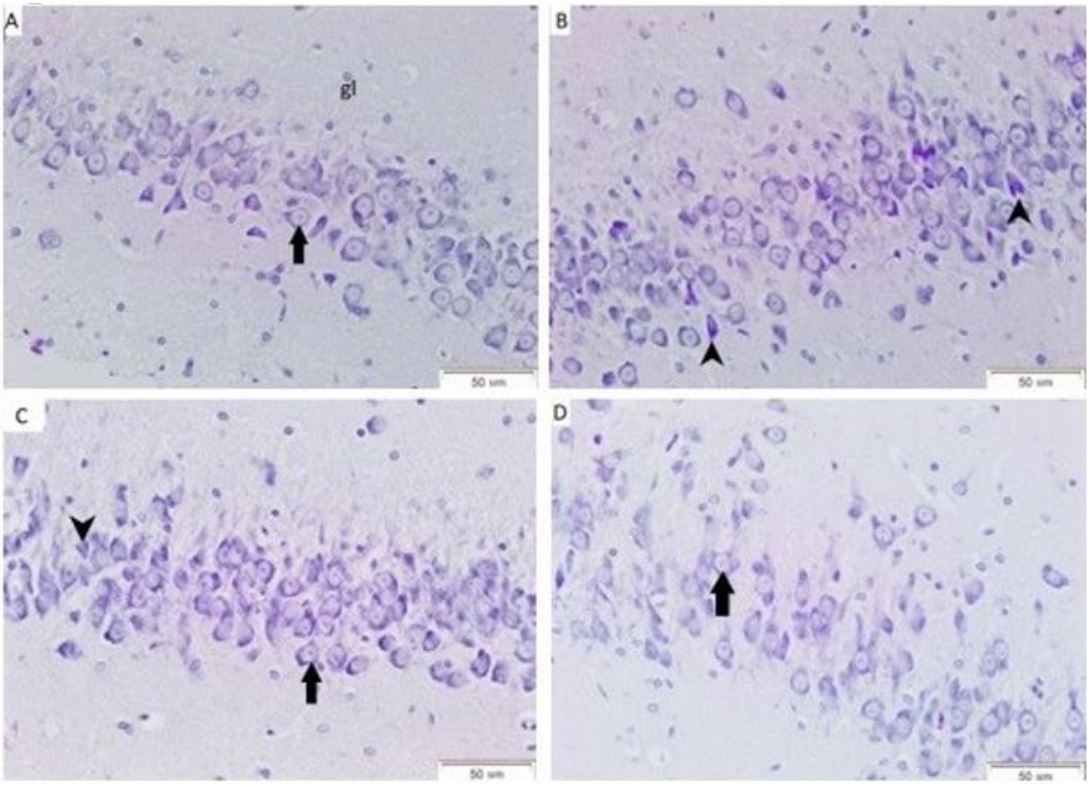

Fig. 4. Toluidine blue-stained coronal sections show large pyramidal cells of CA3 in (A) control, (B) diabetic, (C) treated &(D) exenatide groups respectively (arrows). Note the presence of some darkly-stained shrunken neurons in the diabetic CA3 (arrowheads). (gl) glial cells**.** X400 magnification.

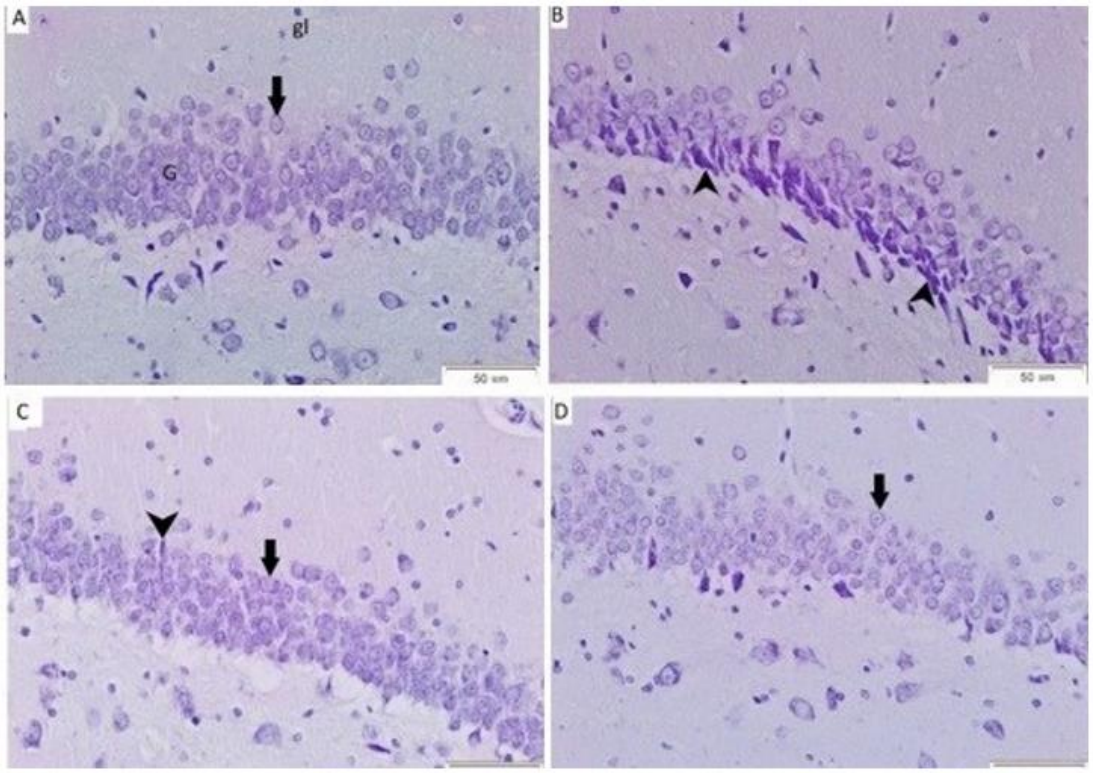

Fig. 5. Toluidine blue-stained coronal sections show small granular cells of DG in (A) control, (B) diabetic, (C) treated &(D) exenatide groups respectively (arrows). Many darkly-stained shrunken neurons are observed in the deeper layers of the granular layer (G) of diabetic DG (arrowheads). (gl) glial cells. X400 magnification.

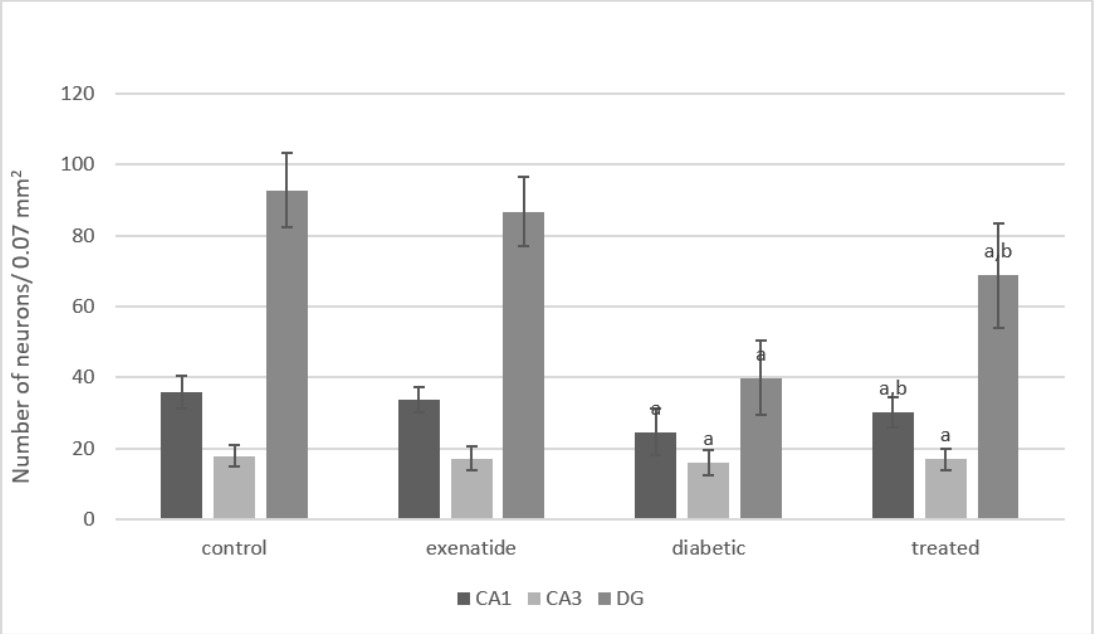

Fig. 6. Mean ±SD values of neuronal cell count in the CA1, CA3, and DG of the hippocampus of different groups. [a] Significantly different from the control group. [b] Significantly different from the diabetic group.

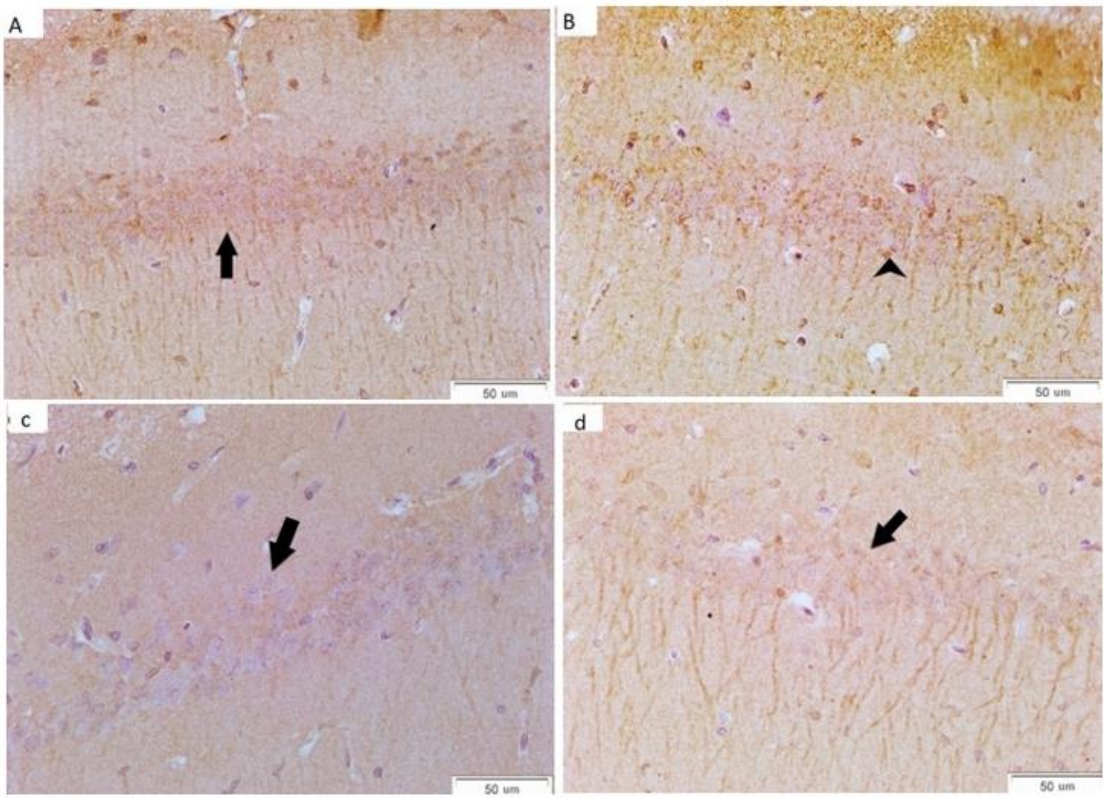

Fig. 7. Rat hippocampal caspase-3 immunohistochemical stain showing the CA1 of (A) control, (B) diabetic, (C) treated & (D) exenatide groups. Arrow points to weak immune-reactivity of neuronal cytoplasm in the control group. Arrowhead points to intense immune-reactivity in many granular cells of the diabetic group. X400 magnification.

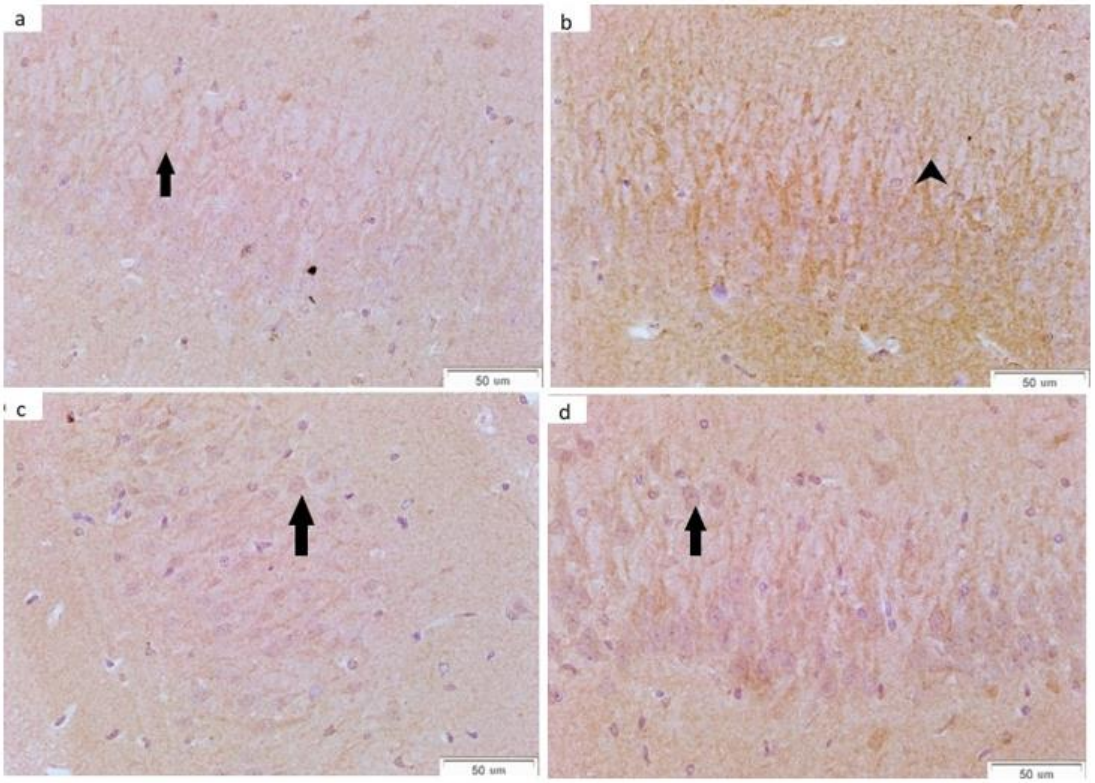

Fig. 8. Rat hippocampal caspase-3 immunohistochemical stain showing the CA3 of (A) control, (B) diabetic, (C) treated & (D) exenatide groups. Arrow points to weak immune-reactivity of neuronal cytoplasm in the control group. Arrowhead points to intense immune-reactivity in many granular cells of the diabetic group. X400 magnification.

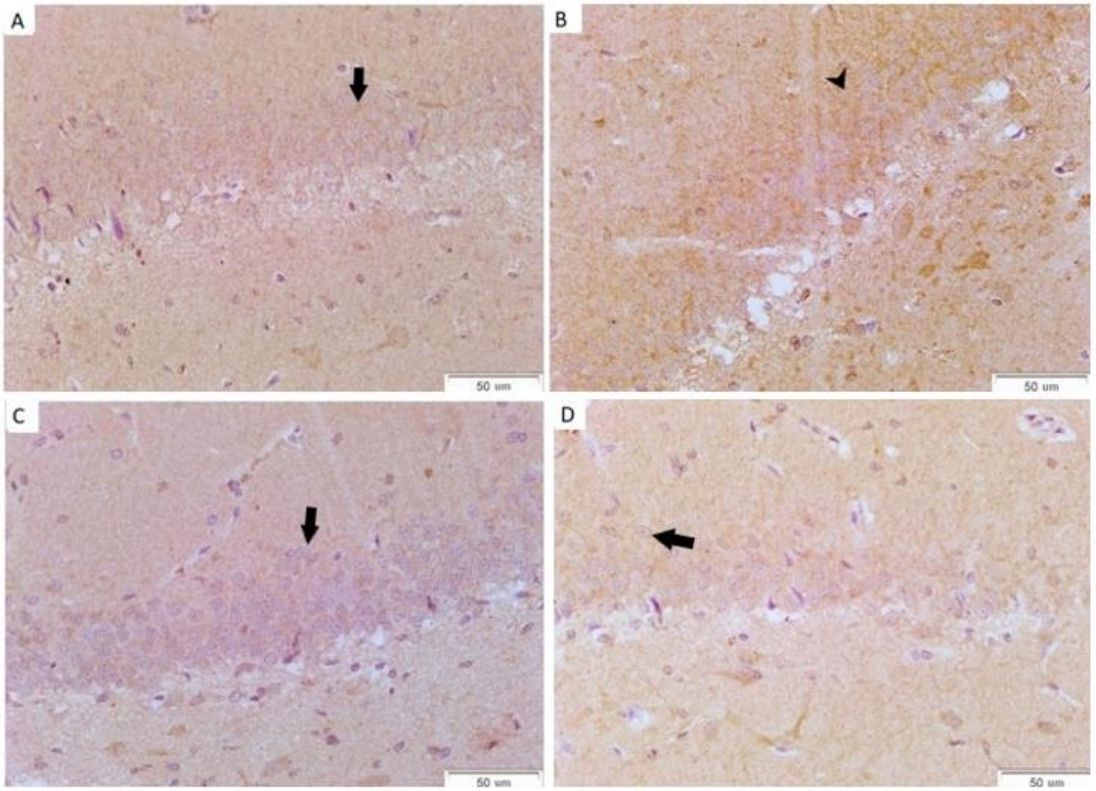

Fig. 9. Rat hippocampal caspase-3 immunohistochemical stain showing the DG of(A) control, (B) diabetic, (C) treated & (D) exenatide groups. Arrow points to weak immune-reactivity of neuronal cytoplasm in the control group. Arrowhead points to intense immune-reactivity in many granular cells of the diabetic group. X400 magnification.

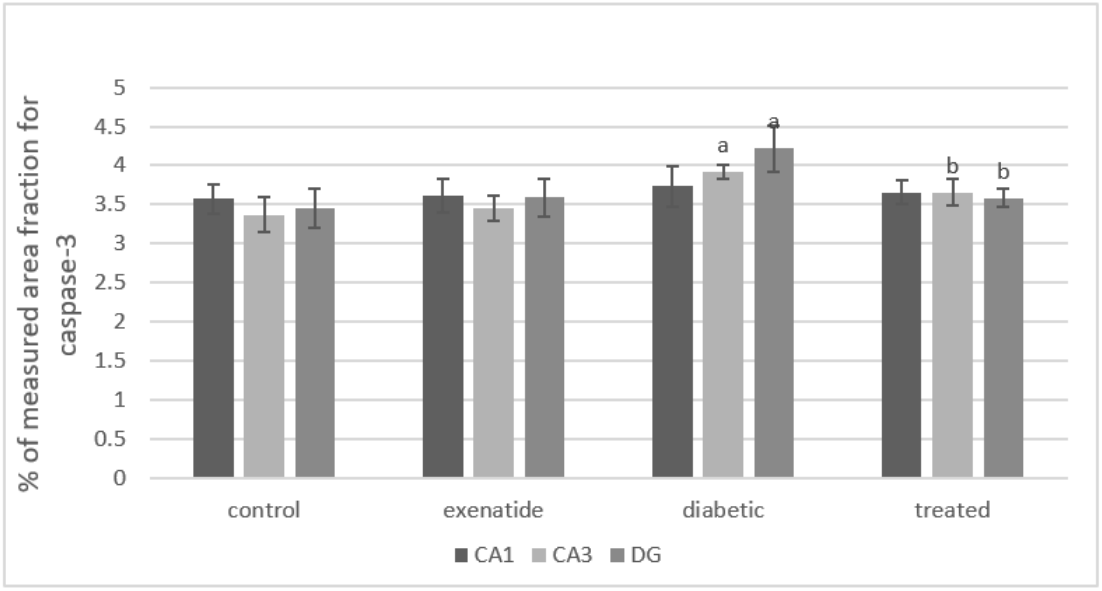

Fig. 10. Mean ±SD values for measured area fraction for the caspase-3 immunohistochemical stain of CA1, CA3 and DG of the hippocampus of different groups. [a] Significantly different from the control group. [b] Significantly different from the diabetic group.

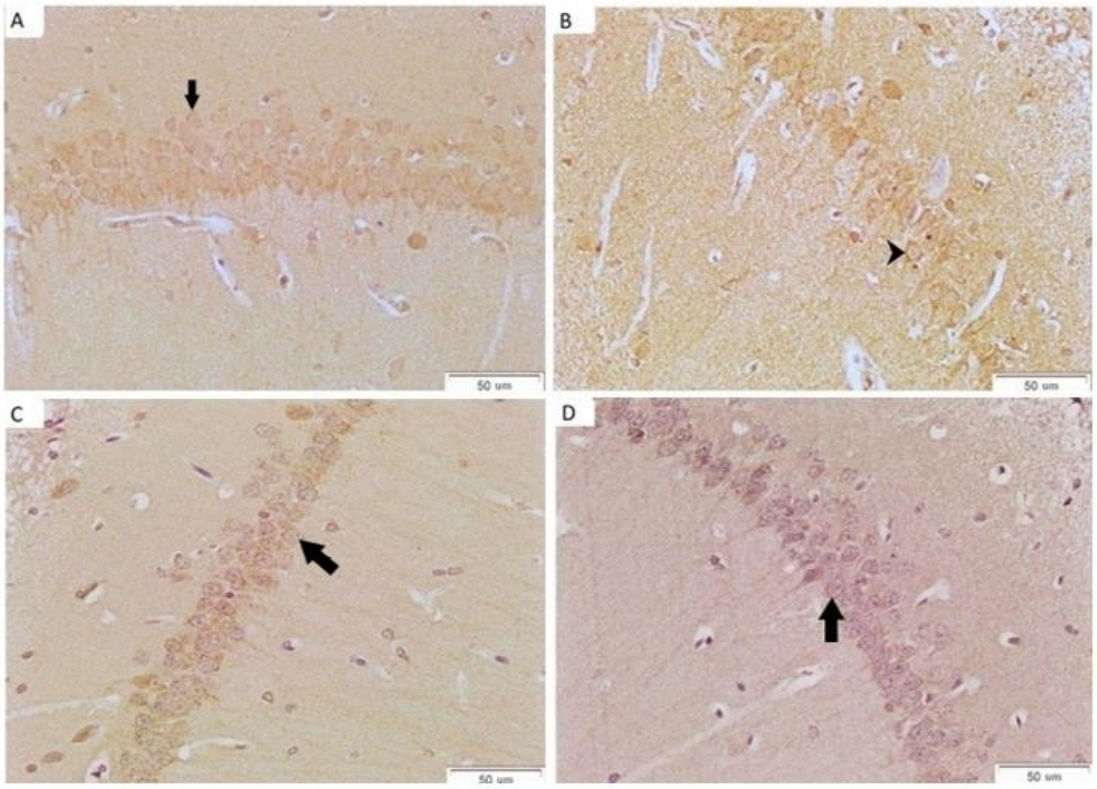

Fig.11. Rat hippocampal LC3b immunohistochemical stain of CA1 in (A) control, (B) diabetic, (C) treated & (D) exenatide groups respectively. (Arrow) points to immune-reactivity of the cytoplasm of neurons in the control group. Arrowhead points to more intense immune-reactivity of the cytoplasm of neurons in the diabetic group. X400 magnification.

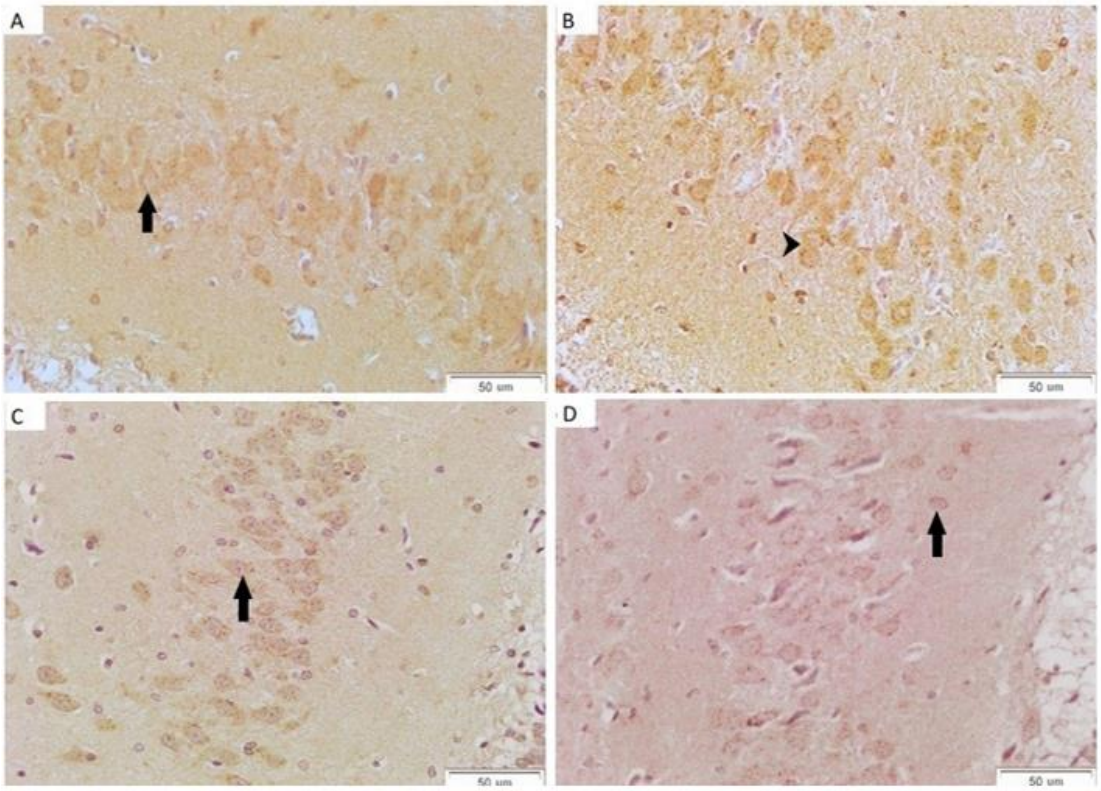

Fig. 12. Rat hippocampal LC3b immunohistochemical stain of CA3 in (A) control, (B) diabetic, (C) treated & (D)exenatide groups. Arrow points to immune-reactivity of the cytoplasm of neurons in the control group. Arrowhead points to more intense immune-reactivity of the cytoplasm of neurons in the diabetic group. X400 magnification.

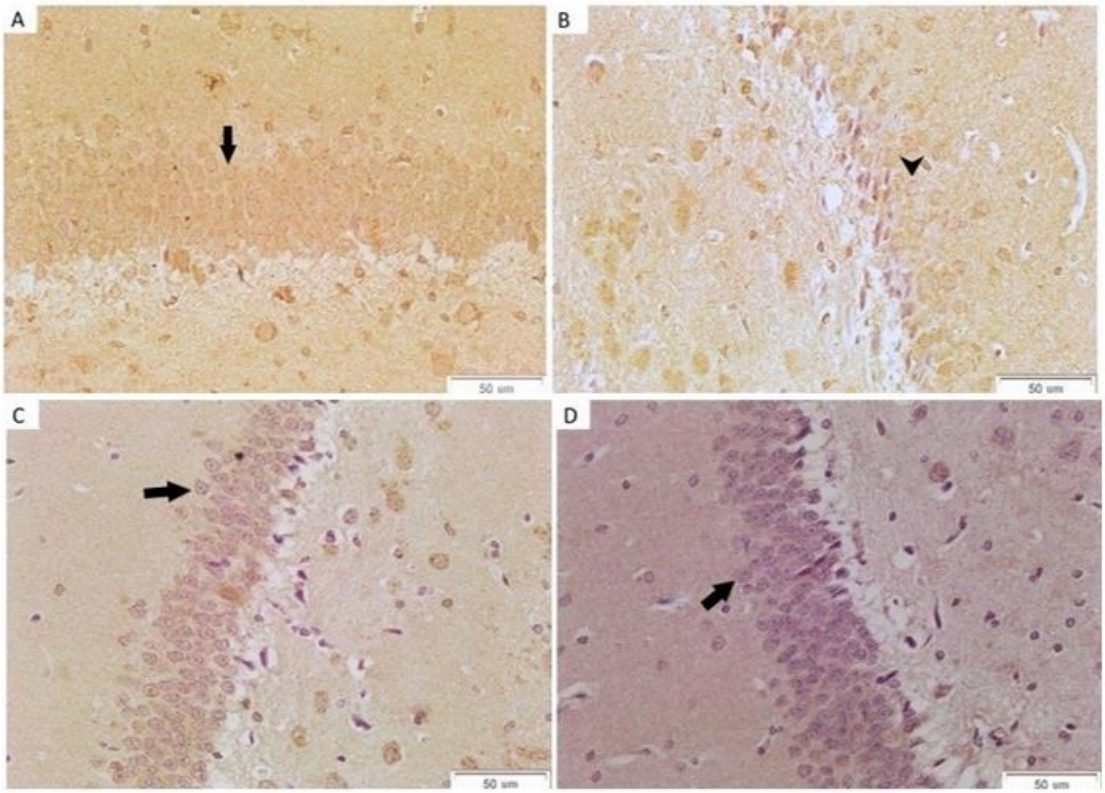

Fig. 13. Rat hippocampal LC3b immunohistochemical stain of DG in (A) control, (B) diabetic, (C) treated & (D) exenatide groups respectively. Arrow points to immune-reactivity of the cytoplasm of neurons in the control group. Arrowhead points to more intense immune-reactivity of the cytoplasm of neurons in the diabetic group. X400 magnification.

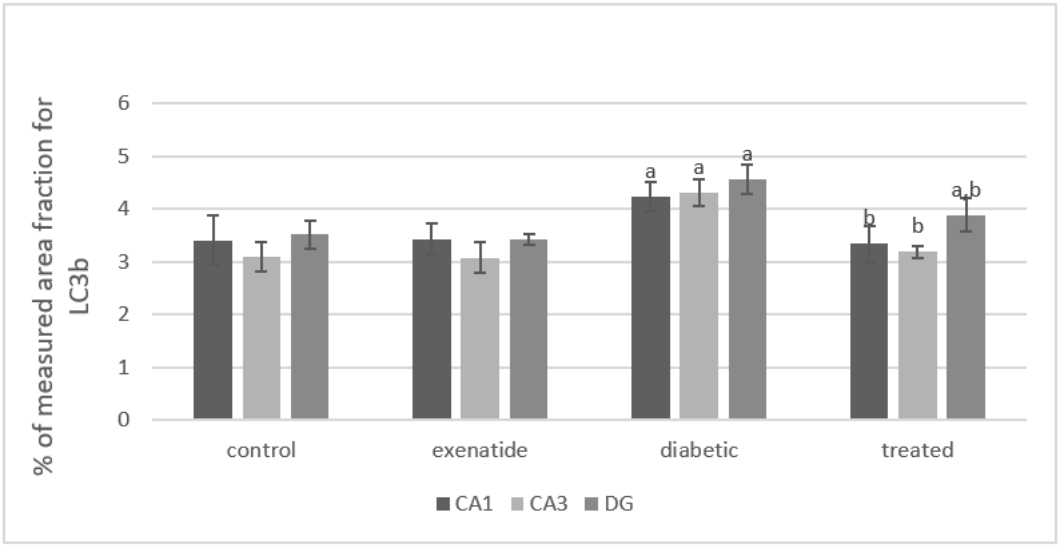

Fig. 14. Mean ±SD values for measured area fraction for LC3b immunohistochemical stain in CA1, CA3, and DG of the different groups. [a] Significantly different from the control group. [b] Significantly different from the diabetic group.

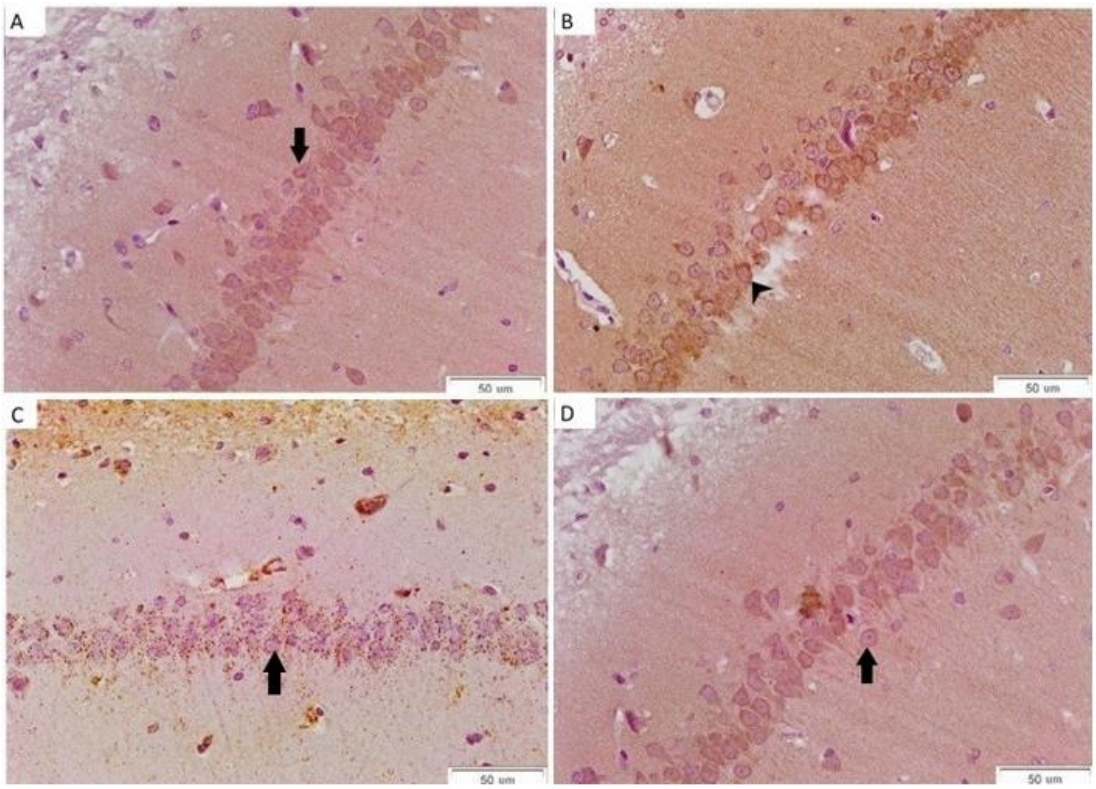

Fig. 15. Rat hippocampal p62 immunohistochemical stain of CA1 in (A) control, (B) diabetic, (C) treated & (D) exenatide groups. Arrow points to weak immune-reactivity of the cytoplasm of neurons in the control group. Arrowhead points to intense immune-reactivity of the cytoplasm of neurons in the diabetic group. X400 magnification

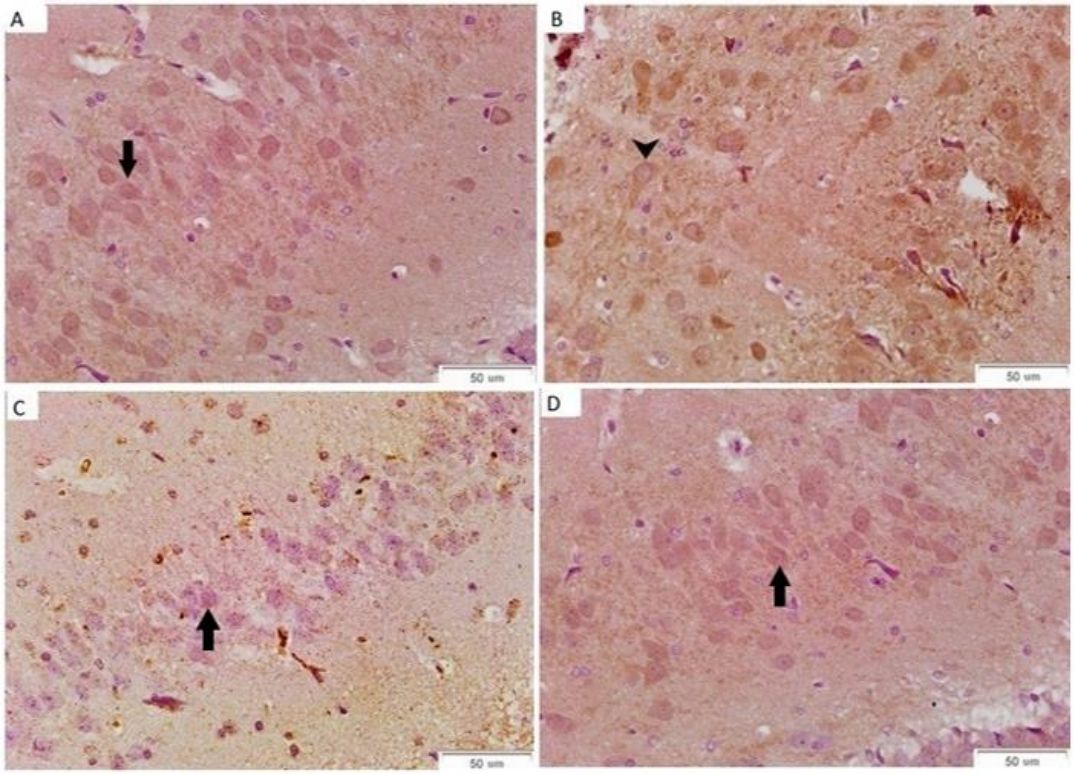

Fig. 16. Rat hippocampal p62 immunohistochemical stain of CA3 in (A) control, (B) diabetic, (C) treated & (D) exenatide groups. Arrow points to weak immune-reactivity of the cytoplasm of neurons in the control group. Arrowhead points to intense immune-reactivity of the cytoplasm of neurons in the diabetic group. X400 magnification

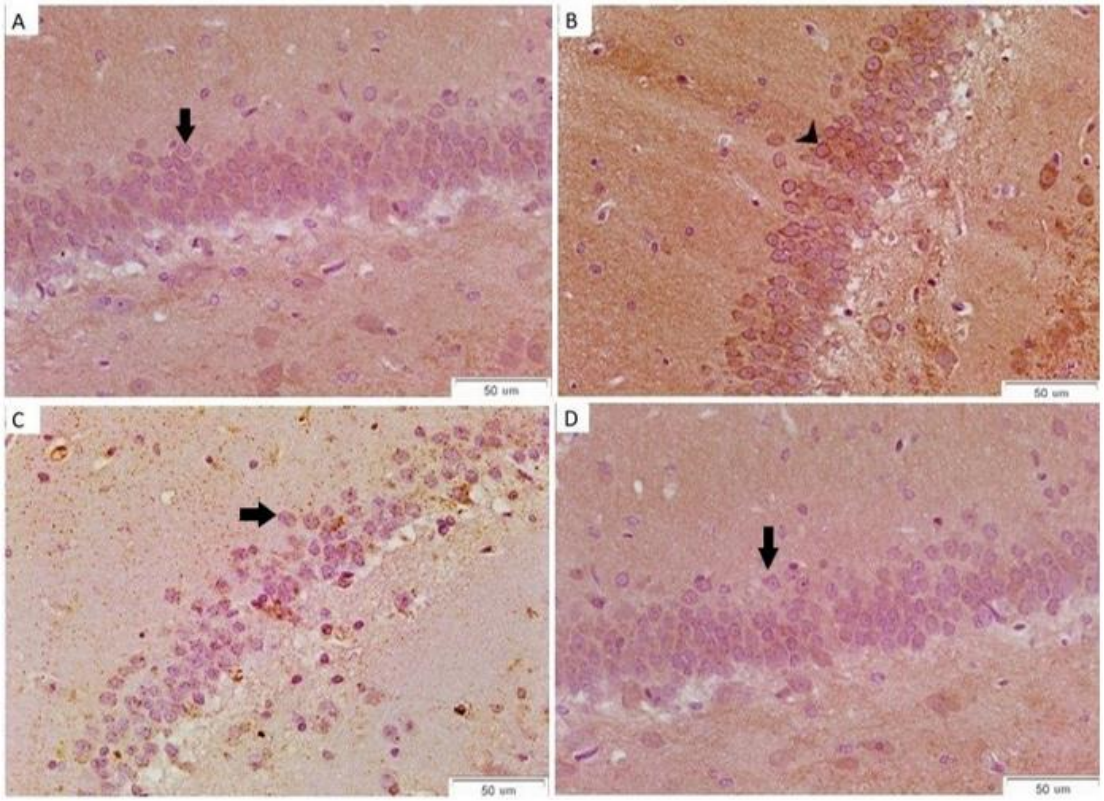

Fig. 17. Rat hippocampal p62 immunohistochemical stain of DG in (A) control, (B) diabetic, (C) treated & (D) exenatide groups. Arrow points to weak immune-reactivity of the cytoplasm of neurons in the control group. Arrowhead points to intense immune-reactivity of the cytoplasm of neurons in the diabetic group. X400 magnification.

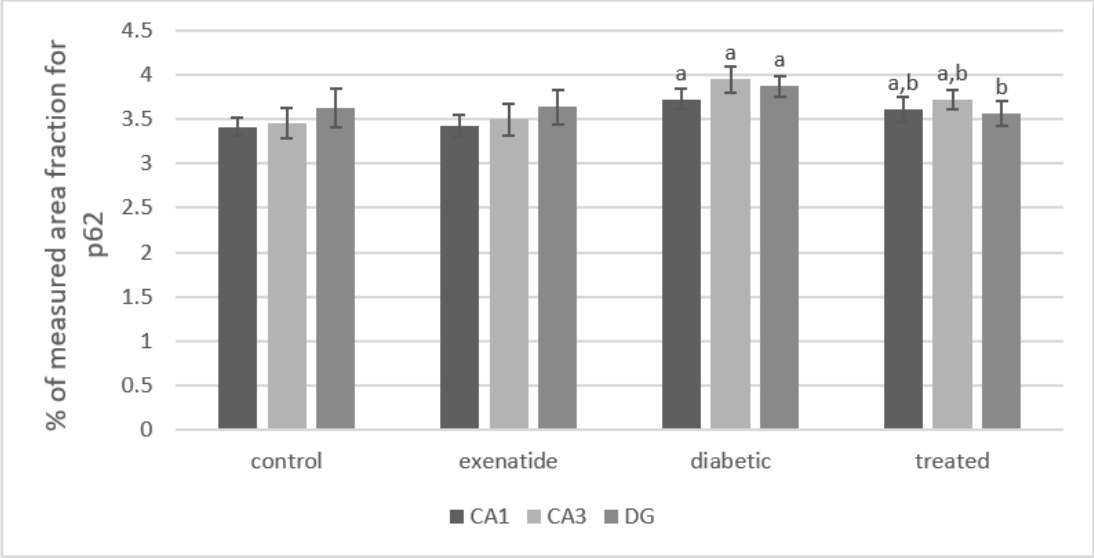

Fig. 18. Mean ±SD values for measured area fraction for p62 immunohistochemical stain in CA1, CA3, and DG of the different groups. [a] Significantly different from the control group. [b] Significantly different from the diabetic group.

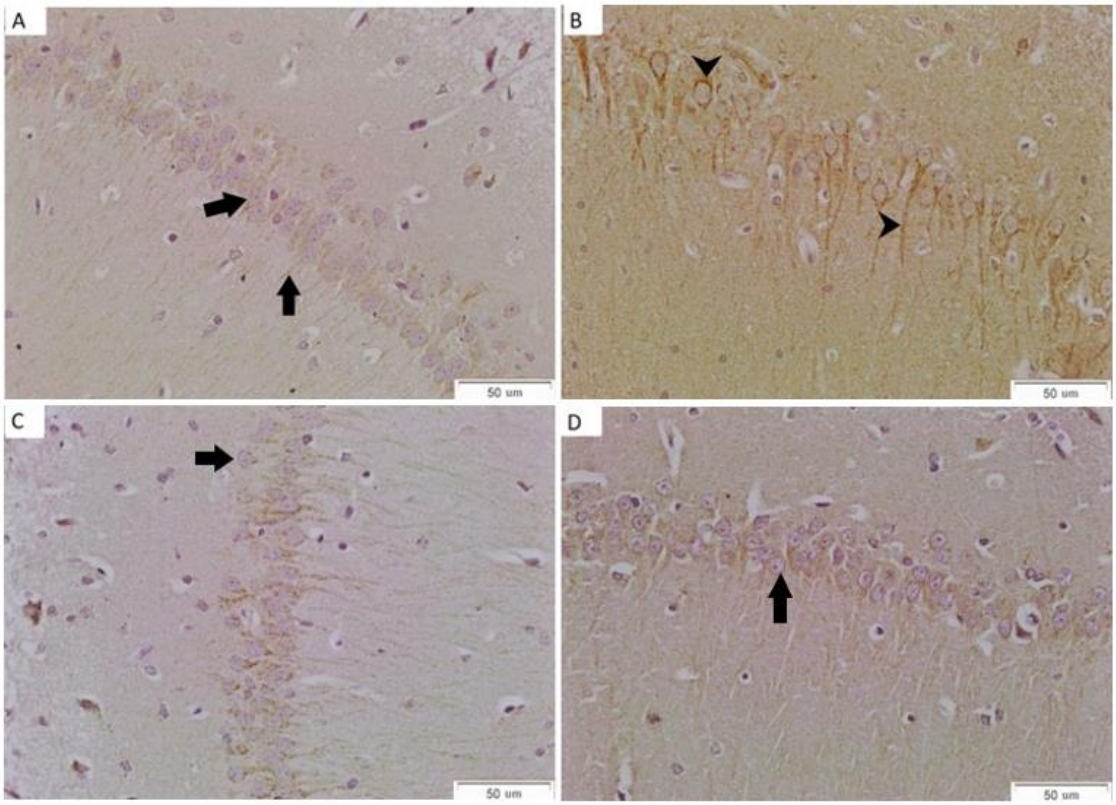

Fig. 19. Rat hippocampal RIP3 immunohistochemical stain showing the CA1 of (A) control, (B) diabetic, (C) treated &(D) exenatide groups. Arrows point to weak immune-reactivity of the cytoplasm of neurons & neuronal processes in the control group. Arrowheads point to intense immune-reactivity of the cytoplasm of neurons & neuronal processes in the diabetic group. X400 magnification.

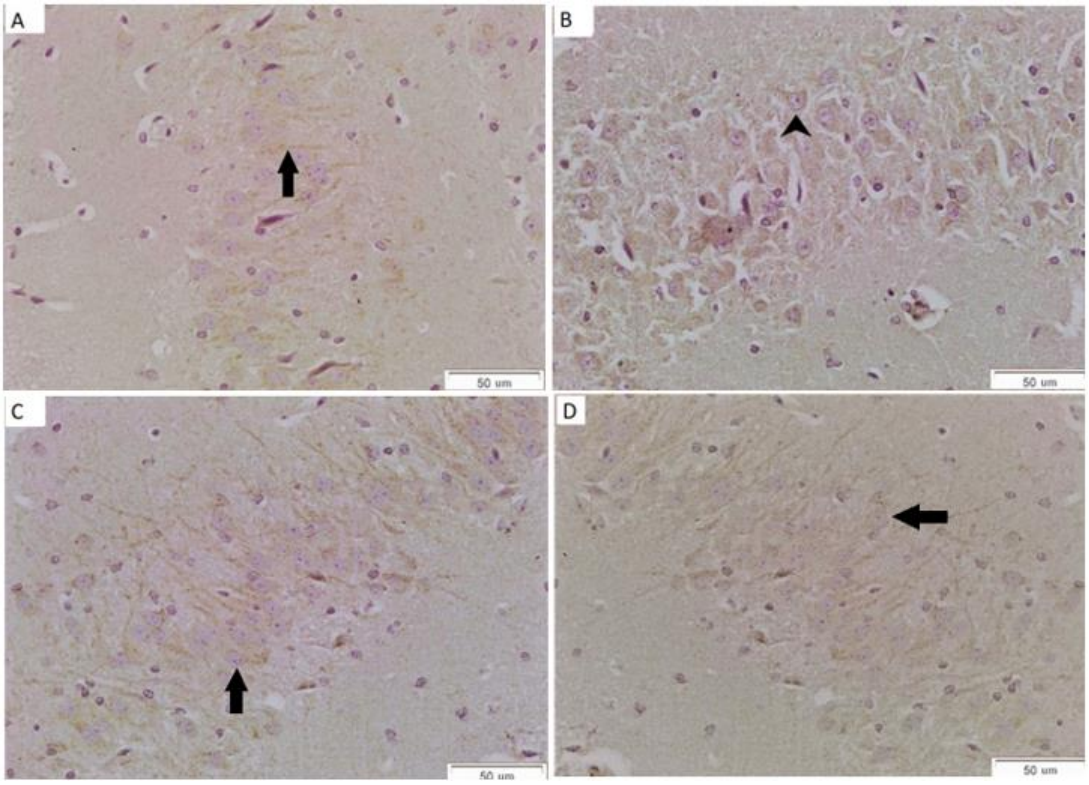

Fig. 20. Rat hippocampal RIP3 immunohistochemical stain showing the CA3 of (A) control, (B) diabetic, (C) treated & (D) exenatide groups. Arrows point to weak immune-reactivity of the cytoplasm of neurons & neuronal processes in the control group. Arrowheads point to relatively similar immune-reactivity of the cytoplasm of neurons & neuronal processes in the diabetic group. X400 magnification**.**

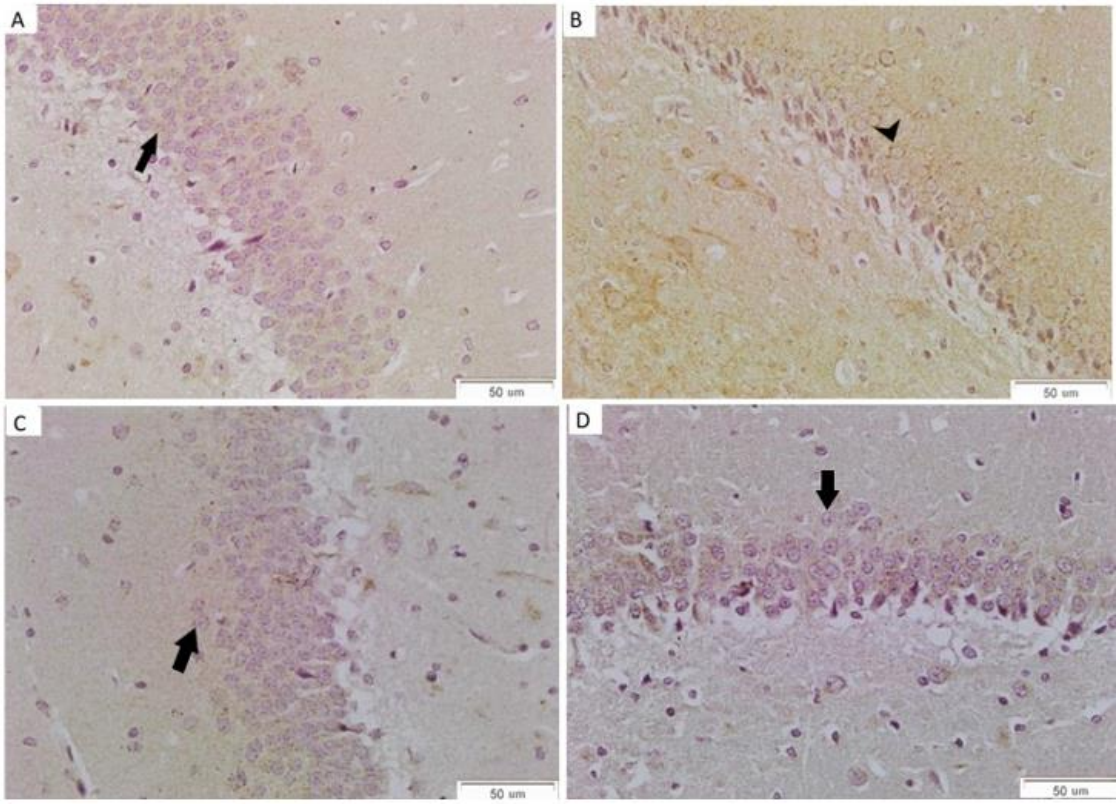

Fig. 21. Rat hippocampal RIP3 immunohistochemical stain showing the DG of (A) control, (B) diabetic, (C) treated &(D) exenatide groups. Arrows point to weak immune-reactivity of the cytoplasm of neurons & neuronal processes in the control group. Arrowheads point to intense immune-reactivity of the cytoplasm of neurons & neuronal processes in the diabetic group. X400 magnification.

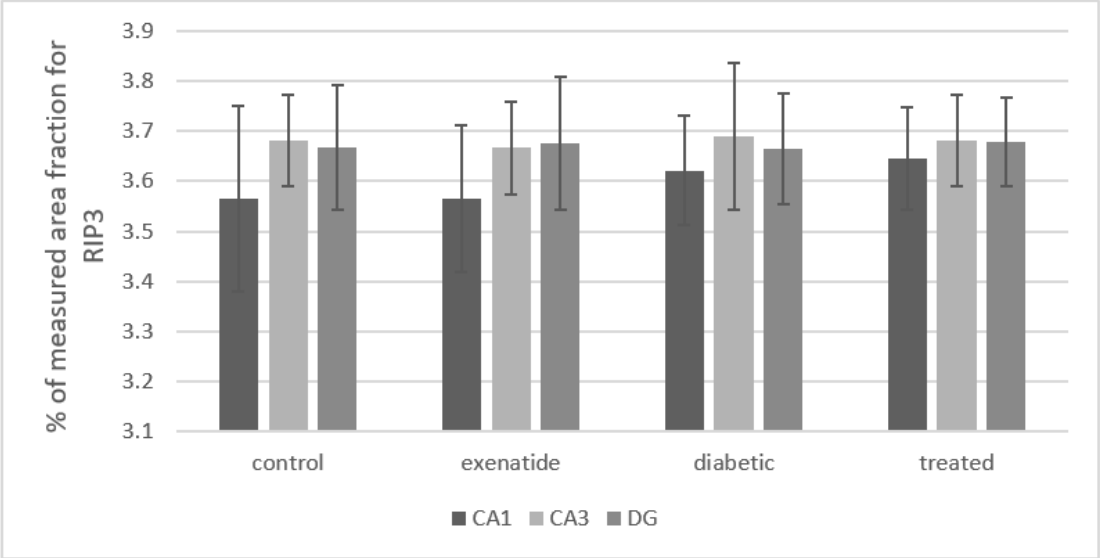

Fig. 22. Mean ±SD values for measured area fraction for RIP3 immunohistochemical stain of CA1, CA3, and DG of the different groups.

DISCUSSION

Hyperglycaemia and related oxidative stress play a pivotal role in the pathogenesis of both types of diabetes mellitus (Oyenihi *et al.,* 2015 & Yonguc *et al.,* 2015), which was evident in the present work. Exenatide treatment improved blood glucose levels as compared to diabetic rats, though not fully controlled as compared to non-diabetic rats. However, exenatide treatment did not produce significant improvement of oxidative stress markers (SOD, MDA & GSH) of the hippocampal homogenates. Although many studies stated that GLP-1 agonists have an antioxidant effect in different diabetic models (Ding et al., 2019 & Elbassuoni and Ahmed, 2019), some reported no lowering effect on ROS levels (Younce *et al.,* 2013). The antioxidant effect of GLP-1 agonists may depend on various factors such as dose, diabetic status, and obesity (Petersen *et al.,* 2016).

There is a cross-regulation between autophagy and apoptosis, as they can work in synergism or antagonize each other. Both work together to dispose of cells secondary to any deleterious insult, as one mechanism leads to cell death and the other one helps or becomes activated if the former one failed. In other conditions with damaged organelles or misfolded proteins, autophagy antagonizes apoptosis and inhibits further activation of it (Demirtas *et al.,* 2016), and inhibition of autophagy may induce neuronal apoptosis (Zhang *et al.,* 2013 & Li *et al.,* 2017).

Autophagic flux is defined as the rate of turnover of autophagic vacuoles (Gukovskaya and Gukovsky, 2012). Microtubule-associated protein Light Chain 3 (LC3) is a key contributor to the conjugation system for autophagosome formation (Huang and Liu, 2015). LC3-II is considered a marker of autophagy formation, as it is associated with the outer and inner membranes of the autophagosome (Lalaoui et al., 2015 & Chen *et al.,* 2018). Another protein important for autophagy is p62 that induces nucleation of the autophagosome membrane, then recruitment of the ubiquitylated proteins and degradation through autophagy (Ichimura and Komatsu, 2010; Sánchez-Martín and Komatsu, 2018). Autophagy activation is associated with a decrease in p62, while an increase in p62 is associated with autophagy inhibition (Ma *et al.,* 2017).

In this study, diabetes increased immune reaction for LC3b in all regions of the hippocampus as compared to the

control group. However, the increase in LC3b was also accompanied by an increase in the immune reaction for p62. So, our results may indicate late-stage inhibition of autophagy, which agrees with (Lalaoui *et al.,* 2015). Many studies revealed that DM is associated with impairment of autophagic flux as has been observed in the hippocampus of diabetic mice and high glucose-treated neurons (Xue *et al.,* 2016 & Yerra and Kumar, 2017)**.** This impairment was related to lysosomal dysfunction (Yuan *et al.,* 2019b). On the contrary, (Wu *et al.,* 2019) reported that diabetes-associated cognitive decline was associated with a significant increase in autophagic activation. (Li *et al.,* 2017) stated that the changes observed in autophagic activity are the net effect of several factors that differs according to the type and pathophysiology of DM, and the metabolic alteration that predominates.

In this work, exenatide treatment significantly reversed the effect of diabetes on the immune expression of LC3b and p62 in all hippocampal regions, which might indicate restoration of the autophagic pathway to some extent. The treated group displayed a significant decrease in p62 expression as compared to the diabetic group, which could be explained by discontinuing the late-stage inhibition and disposing of the accumulated autophagic vacuoles. Candeias *et al.* (2018) found that exendin-4 enhanced the autophagic pathways by inducing the removal of toxic proteins and damaged organelles, as GLP-1 has growth factor-like properties and protects neurons from neurotoxic influences (Gumuslu *et al.,* 2018).

In agreement with previous works (Sadeghi *et al.,* 2016 & Zheng *et al.,* 2016), caspase-3 immune-expression was increased in all hippocampal regions of the diabetic group**.** Caspase-3 is classified as an apoptosis executioner caspase, which is involved in both intrinsic and extrinsic pathways of apoptosis. Hippocampal neuronal loss may be a major contributing mechanism to memory and learning impairments in diabetic animals (Sima et al., 2004). However, Foghi and Ahmadpour (2013) reported no apoptosis in hippocampal pyramidal neurons or any cognitive deficits in 8 weeks diabetic rats**.** Therefore, duration-related apoptosis has been suggested to account for neuronal loss and the concomitant emergence of cognitive impairments in diabetic animals (Sadeghi *et al.,* 2016).

In this study, exenatide treatment reduced apoptosis markedly in the DG region to become almost comparable to that of the control group. During *et al.* (2003) found also that exendin reduced kainite-induced apoptosis of hippocampal neurons**.** Similarly, in type 2 diabetic models, exendin-4 protected against apoptosis via decreasing caspase activities and mitochondrial cytochrome C, in the rat brain cortex (Candeias *et al.,* 2018). On the other hand, autophagy may be involved in exendin-4 anti-apoptotic effects, probably via the reduction of neuronal caspase-3 protein levels (Li *et al.,* 2016).

Importantly, the neuroprotective effects of GLP-1 analogues were also reported to increase neurogenesis (Bertilsson *et al.,* 2008; Harkavyi *et al.,* 2008 & Darsalia *et al.,* 2012). So, the increase in the number of DG neurons observed in this study might be attributed to increased neurogenesis and decreased apoptosis.

Although it is unclear how cells decide which way to die, different studies interpreted that apoptosis is a developmentally programmed cell death required for organismal function, but necroptosis is an ‘emergency’ defensive cell suicide that is involved in limiting pathogen spread and promoting inflammatory and immune responses (Oberst, 2016).

Necroptosis is a form of programmed necrosis that is typically initiated via death receptors, such as Fas

or TNF receptor (Sun *et al.,* 2012), leading to the formation of a necrosome complex, which contains receptor-interacting kinase-1 (RIP1) (Holler *et al.,* 2000), receptor-interacting kinase-3 (RIP3) (He *et al.,* 2009), and mixed lineage kinase domain-like protein (MLKL) (Sun *et al.,* 2012). Although downstream mechanisms mediating the execution of necroptosis remain not clear, the ROS accumulation (Zhang et al., 2009 & He et al., 2011) and calcium influx (Cai *et al.,* 2014) is essential for necroptosis in certain cell lines. A recent hypothesis suggested that caspase-8-related death receptor signaling may negatively regulate necroptosis via active caspase 8, which can cleave necrosis regulators including RIP1, RIP3 (Liu *et al.,* 2014).

In this study, necroptosis was detected in the diabetic group as a positive immune reaction for RIP3 mainly in the CA1 region, and to a lesser extent in DG, although, it was not significant when compared to the control group. This may indicate more susceptibility of CA1 pyramidal neurons to necroptosis than other regions of the hippocampus. However, Nasseri et al. (2020) observed increased levels of the hippocampal RIP1, RIP3, and TNF-α in STZ-induced diabetic rats.

Conclusion:

The present study demonstrated that diabetes significantly increased hippocampal apoptosis, and impaired autophagic activity, while necroptosis was detected but insignificantly. Exenatide treatment decreased apoptosis and restored autophagic activity.

Funding sources: This research did not receive any specific grant from funding agencies in the public, commercial, or not-for-profit sectors.

Conflict of interest: The authors declare that they have no conflict of interest.

Acknowledgments: The authors thank the experimental research center, where this experiment was performed, and the laboratories at the Faculty of Medicine, Mansoura University, Egypt, for their excellent assistance regarding the scientific and technical support throughout the experiment

REFERENCES

Anand, K. S., & Dhikav, V. (2012). Hippocampus in health and disease: An overview. *Annals of Indian Academy of Neurology*, *15*(4), 239.

Baglietto-Vargas, D., Shi, J., Yaeger, D. M., Ager, R., & LaFerla, F. M. (2016). Diabetes and Alzheimer's disease crosstalk. *Neuroscience & Biobehavioral Reviews*, 64, 272-287.

Bertilsson, G., Patrone, C., Zachrisson, O., Andersson, A., Dannaeus, K., Heidrich, J., Kortesmaa, J., Mercer, A., Nielsen, E., & Rönnholm, H. (2008). Peptide hormone exendin-4 stimulates subventricular zone neurogenesis in the adult rodent brain and induces recovery in an animal model of Parkinson's disease. *Journal of neuroscience research*, *86*(2), 326-338.

Buzanovskii, V. (2015). Methods for the determination of glucose in blood. Part 1. *Review Journal of Chemistry*, *5*(1), 30-81.

Cai, Z., Jitkaew, S., Zhao, J., Chiang, H.-C., Choksi, S., Liu, J., Ward, Y., Wu, L.-g., & Liu, Z.-G. (2014). Plasma membrane translocation of trimerized MLKL protein is required for TNF-induced necroptosis. *Nature cell biology*, *16*(1), 55-65.

Candeias, E., Sebastião, I., Cardoso, S., Carvalho, C., Santos, M. S., Oliveira, C. R., Moreira, P. I., & Duarte, A. I. (2018). Brain GLP-1/IGF-1 signaling and autophagy mediate exendin-4 protection against apoptosis in type 2 diabetic rats. *Molecular neurobiology*, *55*(5), 4030-4050.

Chen, J., Kos, R., Garssen, J., & Redegeld, F. (2019). Molecular

Insights into the Mechanism of Necroptosis: The Necrosome as a Potential Therapeutic Target. *Cells*, *8(12)*, 1486.

Chen, Q., Kang, J., & Fu, C. (2018). The independence of and associations among apoptosis, autophagy, and necrosis. *Signal Transduction and Targeted Therapy*, *3*(1), 1-11.

Culling, C. F. A. (2013). *Handbook of histopathological and histochemical techniques: including museum techniques*. Butterworth-Heinemann.

Darsalia, V., Mansouri, S., Ortsäter, H., Olverling, A., Nozadze, N., Kappe, C., Iverfeldt, K., Tracy, L. M., Grankvist, N., & Sjöholm, Å. (2012). Glucagon-like peptide-1 receptor activation reduces ischaemic brain damage following stroke in Type 2 diabetic rats. *Clinical Science*, *122*(10), 473-483.

Davidson, M. B., Bate, G., & Kirkpatrick, P. (2005). Exenatide. *Nature Reviews Drug Discovery*, *4*(9), 713-714.

Demirtas, L., Guclu, A., Erdur, F. M., Akbas, E. M., Ozcicek, A., Onk, D., & Turkmen, K. (2016). Apoptosis, autophagy & endoplasmic reticulum stress in diabetes mellitus. *The Indian journal of medical research*, *144*(4), 515.

Ding, W., Chang, W.-g., Guo, X.-c., Liu, Y., Xiao, D.-d., Ding, D., Wang, J.-x., & Zhang, X.-j. (2019). Exenatide protects against cardiac dysfunction by attenuating oxidative stress in the diabetic mouse heart. *Frontiers in Endocrinology*, *10*, 202.

During, M. J., Cao, L., Zuzga, D. S., Francis, J. S., Fitzsimons, H. L., Jiao, X., Bland, R. J., Klugmann, M., Banks, W. A., & Drucker, D. J. (2003). Glucagon-like peptide-1 receptor is involved in learning and neuroprotection. *Nature Medicine*, *9*(9), 1173-1179.

Elbassuoni, E. A., & Ahmed, R. F. (2019). Mechanism of the neuroprotective effect of GLP-1 in a rat model of Parkinson's with pre-existing diabetes. *Neurochemistry International*, *131*, 104583.

Elmore, S. (2007). Apoptosis: a review of programmed cell death. *Toxicologic Pathology*, *35*(4), 495-516.

Foghi, K., & Ahmadpour, S. (2013). Diabetes mellitus type 1 and neuronal degeneration in ventral and dorsal hippocampus. *Iranian Journal of Pathology*, *9*(1), 33-37.

Forbes, J. M., & Cooper, M. E. (2013). Mechanisms of diabetic complications. *Physiological Reviews*, *93*(1), 137-188.

Fotuhi, M., Do, D., & Jack, C. (2012). Modifiable factors that alter the size of the hippocampus with ageing. *Nature Reviews Neurology*, *8*(4), 189-202.

Gagne, F. (2014). *Biochemical ecotoxicology: principles and methods*. Elsevier.

Gaudieri, P. A., Chen, R., Greer, T. F., & Holmes, C. S. (2008). Cognitive function in children with type 1 diabetes: a meta-analysis. *Diabetes Care*, *31*(9), 1892-1897.

González-Reyes, R., Aliev, G., Ávila-Rodrigues, M., & E Barreto, G. (2016). Alterations in glucose metabolism on cognition: a possible link between diabetes and dementia. *Current Pharmaceutical Design*, *22*(7), 812-818.

Gukovskaya, A. S., & Gukovsky, I. (2012). Autophagy and pancreatitis. *American Journal of Physiology-Gastrointestinal and Liver Physiology*, *303*(9), G993-G1003.

Gumuslu, E., Cine, N., Ertan, M., Mutlu, O., Komsuoglu

Celikyurt, I., & Ulak, G. (2018). Exenatide upregulates gene expression of glucagon-like peptide-1 receptor and nerve growth factor in streptozotocin/nicotinamide-induced diabetic mice. *Fundamental & Clinical Pharmacology*, *32*(2), 174-180.

Hamilton, A., Patterson, S., Porter, D., Gault, V. A., & Holscher, C. (2011). Novel GLP-1 mimetics developed to treat type 2 diabetes promote progenitor cell proliferation in the brain. *Journal of Neuroscience Research*, *89*(4), 481-489.

Harkavyi, A., Abuirmeileh, A., Lever, R., Kingsbury, A. E., Biggs, C. S., & Whitton, P. S. (2008). Glucagon-like peptide 1 receptor stimulation reverses key deficits in distinct rodent models of Parkinson's disease. *Journal of Neuroinflammation*, *5*(1), 1-9.

He, S., Liang, Y., Shao, F., & Wang, X. (2011). Toll-like receptors activate programmed necrosis in macrophages through a receptor-interacting kinase-3–mediated pathway. *Proceedings of the National Academy of Sciences*, *108*(50), 20054-20059.

He, S., Wang, L., Miao, L., Wang, T., Du, F., Zhao, L., & Wang, X. (2009). Receptor interacting protein kinase-3 determines cellular necrotic response to TNF-α. *Cell*, *137*(6), 1100-1111.

Holler, N., Zaru, R., Micheau, O., Thome, M., Attinger, A., Valitutti, S., Bodmer, J.-L., Schneider, P., Seed, B., & Tschopp, J. (2000). Fas triggers an alternative, caspase-8–independent cell death pathway using the kinase RIP as effector molecule. *Nature Immunology*, *1*(6), 489-495.

Huang, R., & Liu, W. (2015). Identifying an essential role of nuclear LC3 for autophagy. *Autophagy*, *11*(5), 852-853.

Ichimura, Y., & Komatsu, M. (2010). Selective degradation of p62 by autophagy. Seminars in immunopathology,

Lalaoui, N., Lindqvist, L. M., Sandow, J. J., & Ekert, P. G. (2015). The molecular relationships between apoptosis, autophagy and necroptosis. Seminars in cell & developmental biology,

Lee, H. J., Seo, H. I., Cha, H. Y., Yang, Y. J., Kwon, S. H., & Yang, S. J. (2018). Diabetes and Alzheimer's disease: mechanisms and nutritional aspects. *Clinical Nutrition Research*, *7*(4), 229.

Li, H.-T., Zhao, X.-Z., Zhang, X.-R., Li, G., Jia, Z.-Q., Sun, P., Wang, J.-Q., Fan, Z.-K., & Lv, G. (2016). Exendin-4 enhances motor function recovery via promotion of autophagy and inhibition of neuronal apoptosis after spinal cord injury in rats. *Molecular Neurobiology*, *53*(6), 4073-4082.

Li, X., Song, D., & Leng, S. X. (2015). Link between type 2 diabetes and Alzheimer’s disease: from epidemiology to mechanism and treatment. *Clinical Interventions In Aging*, *10*, 549.

Li, Y., Zhang, Y., Wang, L., Wang, P., Xue, Y., Li, X., Qiao, X., Zhang, X., Xu, T., & Liu, G. (2017). Autophagy impairment mediated by S-nitrosation of ATG4B leads to neurotoxicity in response to hyperglycemia. *Autophagy*, *13*(7), 1145-1160.

Liu, S., Wang, X., Li, Y., Xu, L., Yu, X., Ge, L., Li, J., Zhu, Y., & He, S. (2014). Necroptosis mediates TNF-induced toxicity of hippocampal neurons. *BioMed Research International*, *2014*.

Lotfy, M., Singh, J., Rashed, H., Tariq, S., Zilahi, E., & Adeghate, E. (2014). Mechanism of the beneficial and protective effects

of exenatide in diabetic rats. *Journal of Endocrinol*ogy, *220*(3), 291-304. https://doi. org/ 10.1530/joe-13-0426

Lu, F.-P., Lin, K.-P., & Kuo, H.-K. (2009). Diabetes and the risk of multi-system aging phenotypes: a systematic review and meta-analysis. *PloS one*, *4*(1), e4144.

Ma, L.-Y., Lv, Y.-L., Huo, K., Liu, J., Shang, S.-H., Fei, Y.-L., Li, Y.-B., Zhao, B.-Y., Wei, M., & Deng, Y.-N. (2017). Autophagy-lysosome dysfunction is involved in Aβ deposition in STZ-induced diabetic rats. *Behavioural Brain Research*, *320*, 484-493.

Maher, P. A., & Schubert, D. R. (2009). Metabolic links between diabetes and Alzheimer's disease. *Expert Review of Neurotherapeutics*, *9*(5), 617-630.

McClean, P. L., Gault, V. A., Harriott, P., & Hölscher, C. (2010). Glucagon-like peptide-1 analogues enhance synaptic plasticity in the brain: a link between diabetes and Alzheimer's disease. *European Journal of Pharmacology*, *630*(1-3), 158-162.

McGhee, D. J., Ritchie, C. W., Zajicek, J. P., & Counsell, C. E. (2016). A review of clinical trial designs used to detect a disease-modifying effect of drug therapy in Alzheimer's disease and Parkinson's disease. *BMC Neurology*, *16*(1), 1-13.

Mostafavinia, A., Amini, A., Ghorishi, S. K., Pouriran, R., & Bayat, M. (2016). The effects of dosage and the routes of administrations of streptozotocin and alloxan on induction rate of typel diabetes mellitus and mortality rate in rats. *Laboratory Animal Research*, *32*(3), 160-165.

Nasseri, B., Zareian, P., & Alizade, H. (2020). Apelin attenuates streptozotocin-induced learning and memory impairment by modulating necroptosis signaling pathway. *International Immunopharmacology*, *84*, 106546.

Oberst, A. (2016). Death in the fast lane: what's next for necroptosis? *The FEBS Journal*, *283*(14), 2616-2625.

Oyenihi, A. B., Ayeleso, A. O., Mukwevho, E., & Masola, B. (2015). Antioxidant strategies in the management of diabetic neuropathy. *Biomed Research International*, *2015*(515042), 515042.

Petersen, K., Rakipovski, G., Raun, K., & Lykkesfeldt, J. (2016). Does glucagon-like peptide-1 ameliorate oxidative stress in diabetes? Evidence-based on experimental and clinical studies. *Current Diabetes Reviews*, *12*(4), 331-358.

Qinna, N. A., & Badwan, A. A. (2015). Impact of streptozotocin on altering normal glucose homeostasis during insulin testing in diabetic rats compared to normoglycemic rats. *Drug Design, Development and Therapy*, *9*, 2515.

Ramos-Vara, J. (2005). Technical aspects of immunohistochemistry. *Veterinary Pathology*, *42*(4), 405-426.

Sadeghi, A., Hami, J., Razavi, S., Esfandiary, E., & Hejazi, Z. (2016). The effect of diabetes mellitus on apoptosis in hippocampus: cellular and molecular aspects. *International Journal of Preventive Medicine*, *7*.

Saeedi, P., Petersohn, I., Salpea, P., Malanda, B., Karuranga, S., Unwin, N., Colagiuri, S., Guariguata, L., Motala, A. A., & Ogurtsova, K. (2019). Global and regional diabetes prevalence estimates for 2019 and projections for 2030 and 2045:

Results from the International Diabetes Federation Diabetes Atlas. *Diabetes Research and Clinical Practice*, *157*, 107843.

Sánchez-Martín, P., & Komatsu, M. (2018). p62/SQSTM1–steering the cell through health and disease. *Journal of Cell Science*, *131*(21).

Sima, A. A., Kamiya, H., & Li, Z. G. (2004). Insulin, C-peptide, hyperglycemia, and central nervous system complications in diabetes. *European Journal of Pharmacology*, *490*(1-3), 187-197.

Singh, R., Letai, A., & Sarosiek, K. (2019). Regulation of apoptosis in health and disease: the balancing act of BCL-2 family proteins. *Nature Reviews Molecular Cell Biology*, *20*(3), 175-193.

Sun, L., Wang, H., Wang, Z., He, S., Chen, S., Liao, D., Wang, L., Yan, J., Liu, W., & Lei, X. (2012). Mixed lineage kinase domain-like protein mediates necrosis signaling downstream of RIP3 kinase. *Cell*, *148*(1-2), 213-227.

Volpe, C. M. O., Villar-Delfino, P. H., Dos Anjos, P. M. F., & Nogueira-Machado, J. A. (2018). Cellular death, reactive oxygen species (ROS) and diabetic complications. *Cell Death & Disease*, *9*(2), 1-9.

Wu, Y., Ye, L., Yuan, Y., Jiang, T., Guo, X., Wang, Z., Xu, K., Xu, Z., Liu, Y., & Zhong, X. (2019). Autophagy activation is associated with neuroprotection in diabetes-associated cognitive decline. *Aging and Disease*, *10*(6), 1233.

Xue, H., Ji, Y., Wei, S., Yu, Y., Yan, X., Liu, S., Zhang, M., Yao, F., Lan, X., & Chen, L. (2016). HGSD attenuates neuronal apoptosis through enhancing neuronal autophagy in the brain of diabetic mice: the role of AMP-activated protein kinase. *Life Sciences*, *153*, 23-34.

Yang, J.-S., Lu, C.-C., Kuo, S.-C., Hsu, Y.-M., Tsai, S.-C., Chen, S.-Y., Chen, Y.-T., Lin, Y.-J., Huang, Y.-C., & Chen, C.-J. (2017). Autophagy and its link to type II diabetes mellitus. *Biomedicine*, *7*(2).

Yerra, V. G., & Kumar, A. (2017). Adenosine monophosphate-activated protein kinase abates hyperglycemia-induced neuronal injury in experimental models of diabetic neuropathy: effects on mitochondrial biogenesis, autophagy and neuroinflammation. *Molecular Neurobiology*, *54*(3), 2301-2312.

Yonguc, G. N., Dodurga, Y., Adiguzel, E., Gundogdu, G., Kucukatay, V., Ozbal, S., Yilmaz, I., Cankurt, U., Yilmaz, Y., & Akdogan, I. (2015). Grape seed extract has superior beneficial effects than vitamin E on oxidative stress and apoptosis in the hippocampus of streptozotocin-induced diabetic rats. *Gene*, *555*(2), 119-126.

Younce, C. W., Burmeister, M. A., & Ayala, J. E. (2013). Exendin-4 attenuates high glucose-induced cardiomyocyte apoptosis via inhibition of endoplasmic reticulum stress and activation of SERCA2a. *American Journal of Physiology-Cell Physiology*, *304*(6), C508-C518.

Yuan, J., Amin, P., & Ofengeim, D. (2019a). Necroptosis and RIPK1-mediated neuroinflammation in CNS diseases. *Nature Reviews Neuroscience*, *20*(1), 19-33.

Yuan, Y., Chen, Y., Peng, T., Li, L., Zhu, W., Liu, F., Liu, S., An, X., Luo, R., & Cheng, J. (2019b). Mitochondrial ROS-induced lysosomal dysfunction impairs autophagic flux and contributes to M1 macrophage polarization

in a diabetic condition. *Clinical Science*, *133*(15), 1759-1777.

Zhang, D.-W., Shao, J., Lin, J., Zhang, N., Lu, B.-J., Lin, S.-C., Dong, M.-Q., & Han, J. (2009). RIP3, an energy metabolism regulator that switches TNF-induced cell death from apoptosis to necrosis. *Science*, *325*(5938), 332-336.

Zhang, X., Xu, L., He, D., & Ling, S. (2013). Endoplasmic reticulum stress-mediated hippocampal neuron apoptosis involved in diabetic cognitive impairment. *BioMed Research International*, *2013*.

Zhang, Y., Chen, X., Gueydan, C., & Han, J. (2018). Plasma membrane changes during programmed cell deaths. *Cell Research*, *28*(1), 9-21.

Zheng, Y., Yang, Y., Dong, B., Zheng, H., Lin, X., Du, Y., Li, X., Zhao, L., & Gao, H. (2016). Metabonomic profiles delineate potential role of glutamate-glutamine cycle in db/db mice with diabetes-associated cognitive decline. *Molecular Brain*, *9*(1), 1-9.

ARABIC SUMMARY

تأثير الاكزيناتيد على موت الخلايا المبرمج والالتهام الذاتى والتنخر المبرمج فى خلايا قرن آمون فى إناث الفئران المصابة بمرض السكرى

إيمان محمد السعيد السعيد[1], أحمد جمال عبد الغفور حمد[2], أمنية سمير عبد السلام[2], منى عبد الرحيم الشحات[2], فتحى عبد الغنى إبراهيم[2]

1 قسم التشريح الآدمى وعلم الأجنة، كلية الطب، جامعة بورسعيد
2 قسم التشريح الآدمى وعلم الأجنة، كلية الطب، جامعة المنصورة

يهدف هذا البحث إلى معرفة تأثير الاكزيناتيد على الضرر الناتج عن عقارالاستريبتوزوتوسين خاصة علي الآليات المختلفة لموت الخلايا فى النسيج العصبى المعروف بقرن آمون للفئران.

تصميم التجربة:

تم استخدام 24 من إناث الفئران البيضاء البالغين، وتم تقسيمهم إلى 4 مجموعات كالتالى:

1. المجموعة الاولى (المجموعة الضابطة): تحتوي على 6 فئران وستحقن داخل البريتون بمحلول ملحي

2. المجموعة الثانية (مجموعة السكرى): تحتوي على 6 فئران وستحقن داخل البريتون بعقارالاستريبتوزوتوسين مرة واحدة بجرعة 45 مجم/كجم

3. المجموعة الثالثة (مجموعة السكرى+الاكزيناتيد): تحتوي على 6 فئران وستحقن داخل البريتون بعقارالاستريبتوزوتوسين مرة واحدة بجرعة 45 مجم/كجم وبعد 5 ايام بعد التأكد من حدوث السكرى ستحقن داخل البريتون بالاكزيناتيد مرة يوميا بجرعة 1 ميكروجرام/كجم لمدة 10 اسابيع

4. المجموعة الرابعة (مجموعة الاكزيناتيد): تحتوي على 6 فئران وستحقن داخل البريتون بالاكزيناتيد مذاب فى محلول ملحي مرة يوميا بجرعة 1 ميكروجرام/كجم

المواد والطرق البحثية المستخدمة:

فى الوقت المحدد للتجربة تم الحصول على العينات اللازمة وهى :

*عينة من الدم لقياس الجلوكوز لتأكيد السكرى

*عينة من النسيج العصبى قرن آمون لقياس دلالات الاكسدة

*عينة من النسيج العصبى قرن آمون لصبغها بصبغات دلالات آليات موت الخلايا المختلفة مثل الالتهام الذاتى وموت الخلايا المبرمج والتنخر المبرمج.

التحليل الإحصائى:

تم تجميع النتائج وتحليلها عن طريق نظام التحليل الإحصائى SPSS الإصدار20.

النتائج:

- تم تأكيد الإصابة بالسكرى فى كلا المجموعتين الثانية والثالثة بعد 5 أيام من الحقن بعقارالاستريبتوزوتوسين.
- أدى استخدام عقارالاستريبتوزوتوسين إلى زيادة معدلات دلالات الأكسدة فى مجموعة السكرى، مع ملاحظة أن استخدام الاكزيناتيد فى المجموعة الثالثة لم يظهر تحسن ملحوظ فى هذه الدلالات.
- الإصابة بالسكرى نتيجة عقارالاستريبتوزوتوسين أدت إلى زيادة ملحوظة فى الدلالات الخاصة بموت الخلايا المبرمج والالتهام الذاتى، وزيادة طفيفة فى الدلالات الخاصة بالتنخر المبرمج.
- استخدام الاكزيناتيد أدى إلى تحسن ملحوظ فى دلالات موت الخلايا المبرمج والالتهام الذاتى، ولم يكن له تأثير واضح على الدلالات الخاصة بالتنخر المبرمج.